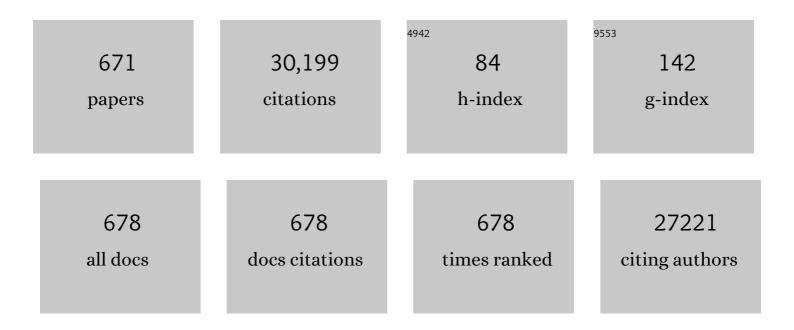
List of Publications by Year in descending order

Source: https://exaly.com/author-pdf/3958337/publications.pdf Version: 2024-02-01



#	Article	IF	CITATIONS
1	Gas molecule adsorption in carbon nanotubes and nanotube bundles. Nanotechnology, 2002, 13, 195-200.	1.3	1,076
2	Rise of silicene: A competitive 2D material. Progress in Materials Science, 2016, 83, 24-151.	16.0	713
3	Metal–Organicâ€Frameworkâ€Derived Hybrid Carbon Nanocages as a Bifunctional Electrocatalyst for Oxygen Reduction and Evolution. Advanced Materials, 2017, 29, 1700874.	11.1	678
4	Atomic-level insight into super-efficient electrocatalytic oxygen evolution on iron and vanadium co-doped nickel (oxy)hydroxide. Nature Communications, 2018, 9, 2885.	5.8	669
5	Facile Ammonia Synthesis from Electrocatalytic N ₂ Reduction under Ambient Conditions on N-Doped Porous Carbon. ACS Catalysis, 2018, 8, 1186-1191.	5.5	520
6	Graphene oxide: A promising nanomaterial for energy and environmental applications. Nano Energy, 2015, 16, 488-515.	8.2	518
7	Boosting electrocatalytic oxygen evolution by synergistically coupling layered double hydroxide with MXene. Nano Energy, 2018, 44, 181-190.	8.2	458
8	Density-functional study ofAun(n=2–20)clusters: Lowest-energy structures and electronic properties. Physical Review B, 2002, 66, .	1.1	425
9	Graphene Nucleation on Transition Metal Surface: Structure Transformation and Role of the Metal Step Edge. Journal of the American Chemical Society, 2011, 133, 5009-5015.	6.6	315
10	Enhanced piezoelectric effect in Janus group-III chalcogenide monolayers. Applied Physics Letters, 2017, 110, .	1.5	307
11	First-Principles Study of Li-Intercalated Carbon Nanotube Ropes. Physical Review Letters, 2000, 85, 1706-1709.	2.9	298
12	Electronic Properties of Carbon Nanotubes with Covalent Sidewall Functionalization. Journal of Physical Chemistry B, 2004, 108, 4227-4230.	1.2	283
13	Noncovalent functionalization of carbon nanotubes by aromatic organic molecules. Applied Physics Letters, 2003, 82, 3746-3748.	1.5	260
14	Mechanical properties of graphene oxides. Nanoscale, 2012, 4, 5910.	2.8	239
15	Silicene on Substrates: A Way To Preserve or Tune Its Electronic Properties. Journal of Physical Chemistry C, 2013, 117, 10353-10359.	1.5	237
16	Structures, mobilities, electronic and magnetic properties of point defects in silicene. Nanoscale, 2013, 5, 9785.	2.8	230
17	2D covalent triazine framework: a new class of organic photocatalyst for water splitting. Journal of Materials Chemistry A, 2015, 3, 7750-7758.	5.2	229
18	Ultrasensitive Ironâ€Triggered Nanosized Fe–CoOOH Integrated with Graphene for Highly Efficient Oxygen Evolution. Advanced Energy Materials, 2017, 7, 1602148.	10.2	216

#	Article	IF	CITATIONS
19	Heterostructures of MXenes and N-doped graphene as highly active bifunctional electrocatalysts. Nanoscale, 2018, 10, 10876-10883.	2.8	215
20	Effects of Sidewall Functionalization on Conducting Properties of Single Wall Carbon Nanotubes. Nano Letters, 2006, 6, 916-919.	4.5	213
21	First-principles calculations of second- and third-order elastic constants for single crystals of arbitrary symmetry. Physical Review B, 2007, 75, .	1.1	210
22	From Boron Cluster to Two-Dimensional Boron Sheet on Cu(111) Surface: Growth Mechanism and Hole Formation. Scientific Reports, 2013, 3, 3238.	1.6	206
23	Recent progress on 2D magnets: Fundamental mechanism, structural design and modification. Applied Physics Reviews, 2021, 8, .	5.5	202
24	Exceptional Electrochemical HER Performance with Enhanced Electron Transfer between Ru Nanoparticles and Single Atoms Dispersed on a Carbon Substrate. Angewandte Chemie - International Edition, 2021, 60, 16044-16050.	7.2	200
25	Magnetism of Transition-Metal/Carbon-Nanotube Hybrid Structures. Physical Review Letters, 2003, 90, 257203.	2.9	198
26	Intrinsic Strength and Failure Behaviors of Graphene Grain Boundaries. ACS Nano, 2012, 6, 2704-2711.	7.3	197
27	Engineering Multifunctional Collaborative Catalytic Interface Enabling Efficient Hydrogen Evolution in All pH Range and Seawater. Advanced Energy Materials, 2019, 9, 1901333.	10.2	196
28	Fe-Anchored Graphene Oxide: A Low-Cost and Easily Accessible Catalyst for Low-Temperature CO Oxidation. Journal of Physical Chemistry C, 2012, 116, 2507-2514.	1.5	189
29	Novel Structures and Properties of Gold Nanowires. Physical Review Letters, 2001, 86, 2046-2049.	2.9	186
30	Work functions of pristine and alkali-metal intercalated carbon nanotubes and bundles. Physical Review B, 2002, 65, .	1.1	183
31	Initial geometries, interaction mechanism and high stability of silicene on Ag(111) surface. Scientific Reports, 2012, 2, 861.	1.6	183
32	Atomistic insight into the oxidation of monolayer transition metal dichalcogenides: from structures to electronic properties. RSC Advances, 2015, 5, 17572-17581.	1.7	183
33	MBene (MnB): a new type of 2D metallic ferromagnet with high Curie temperature. Nanoscale Horizons, 2018, 3, 335-341.	4.1	183
34	Tuning the Band Gap in Silicene by Oxidation. ACS Nano, 2014, 8, 10019-10025.	7.3	175
35	Rapid and energy-efficient microwave pyrolysis for high-yield production of highly-active bifunctional electrocatalysts for water splitting. Energy and Environmental Science, 2020, 13, 545-553.	15.6	169
36	Band Gap Tuning of Hydrogenated Graphene: H Coverage and Configuration Dependence. Journal of Physical Chemistry C, 2011, 115, 3236-3242.	1.5	167

#	Article	IF	CITATIONS
37	Screening and Design of Novel 2D Ferromagnetic Materials with High Curie Temperature above Room Temperature. ACS Applied Materials & Interfaces, 2018, 10, 39032-39039.	4.0	167
38	Probing the Electronic Effect of Carbon Nanotubes in Catalysis: NH ₃ Synthesis with Ru Nanoparticles. Chemistry - A European Journal, 2010, 16, 5379-5384.	1.7	164
39	Endohedrally Doped Cage Clusters. Chemical Reviews, 2020, 120, 9021-9163.	23.0	164
40	Correlation between hardness and elastic moduli of the covalent crystals. Computational Materials Science, 2011, 50, 2287-2290.	1.4	163
41	Comparative Study of Hydrogen Adsorption on Carbon and BN Nanotubes. Journal of Physical Chemistry B, 2006, 110, 13363-13369.	1.2	157
42	Structural Growth Sequences and Electronic Properties of Zinc Oxide Clusters (ZnO)n(n=2-18). Journal of Physical Chemistry C, 2007, 111, 4956-4963.	1.5	157
43	Ultrahigh Rate and Longâ€Life Sodiumâ€Ion Batteries Enabled by Engineered Surface and Nearâ€Surface Reactions. Advanced Materials, 2018, 30, 1702486.	11.1	153
44	B80 and B101–103 clusters: Remarkable stability of the core-shell structures established by validated density functionals. Journal of Chemical Physics, 2012, 136, 074302.	1.2	150
45	Multilevel Hollow MXene Tailored Lowâ€Pt Catalyst for Efficient Hydrogen Evolution in Fullâ€pH Range and Seawater. Advanced Functional Materials, 2020, 30, 1910028.	7.8	150
46	Chemical environment and magnetic moment effects on point defect formations in CoCrNi-based concentrated solid-solution alloys. Acta Materialia, 2020, 187, 122-134.	3.8	149
47	Structure and electronic properties ofGen(n=2–25)clusters from density-functional theory. Physical Review B, 2001, 64, .	1.1	147
48	B ₈₀ and Other Medium-Sized Boron Clusters: Coreâ^'Shell Structures, Not Hollow Cages. Journal of Physical Chemistry A, 2010, 114, 9969-9972.	1.1	143
49	Magic Carbon Clusters in the Chemical Vapor Deposition Growth of Graphene. Journal of the American Chemical Society, 2012, 134, 2970-2975.	6.6	138
50	Quasi-freestanding epitaxial silicene on Ag(111) by oxygen intercalation. Science Advances, 2016, 2, e1600067.	4.7	138
51	In situ capture of active species and oxidation mechanism of RhB and MB dyes over sunlight-driven Ag/Ag3PO4 plasmonic nanocatalyst. Applied Catalysis B: Environmental, 2012, 125, 538-545.	10.8	137
52	Structures and electronic properties of Cu20, Ag20, and Au20 clusters with density functional method. Chemical Physics Letters, 2003, 380, 716-720.	1.2	129
53	Endohedral Silicon Fullerenes SiN(27 ≤≤39). Journal of the American Chemical Society, 2004, 126, 13845-13849.	6.6	129
54	Hole Defects and Nitrogen Doping in Graphene: Implication for Supercapacitor Applications. ACS Applied Materials & Interfaces, 2013, 5, 11184-11193.	4.0	128

#	Article	IF	CITATIONS
55	Nitrogen-Doped Graphene on Transition Metal Substrates as Efficient Bifunctional Catalysts for Oxygen Reduction and Oxygen Evolution Reactions. ACS Applied Materials & Interfaces, 2017, 9, 22578-22587.	4.0	128
56	Transition Metal Surface Passivation Induced Graphene Edge Reconstruction. Journal of the American Chemical Society, 2012, 134, 6204-6209.	6.6	127
57	2D Boron Sheets: Structure, Growth, and Electronic and Thermal Transport Properties. Advanced Functional Materials, 2020, 30, 1904349.	7.8	124
58	YN2 monolayer: Novel p-state Dirac half metal for high-speed spintronics. Nano Research, 2017, 10, 1972-1979.	5.8	120
59	Formation of Carbon Clusters in the Initial Stage of Chemical Vapor Deposition Graphene Growth on Ni(111) Surface. Journal of Physical Chemistry C, 2011, 115, 17695-17703.	1.5	119
60	Oxidation Resistance of Monolayer Group-IV Monochalcogenides. ACS Applied Materials & Interfaces, 2017, 9, 12013-12020.	4.0	118
61	Do Composite Single-Walled Nanotubes Have Enhanced Capability for Lithium Storage?. Chemistry of Materials, 2005, 17, 992-1000.	3.2	117
62	Graphene oxide as a chemically tunable 2-D material for visible-light photocatalyst applications. Journal of Catalysis, 2013, 299, 204-209.	3.1	115
63	Amorphous structural models for graphene oxides. Carbon, 2012, 50, 1690-1698.	5.4	114
64	MBenes: emerging 2D materials as efficient electrocatalysts for the nitrogen reduction reaction. Nanoscale Horizons, 2020, 5, 1106-1115.	4.1	114
65	Appropriate description of intermolecular interactions in the methane hydrates: An assessment of DFT methods. Journal of Computational Chemistry, 2013, 34, 121-131.	1.5	111
66	Melting behavior in ultrathin metallic nanowires. Physical Review B, 2002, 66, .	1.1	105
67	Boron Nitride Nanotubes for Ammonia Synthesis: Activation by Filling Transition Metals. Journal of the American Chemical Society, 2020, 142, 308-317.	6.6	105
68	Binding energies and electronic structures of adsorbed titanium chains on carbon nanotubes. Physical Review B, 2002, 66, .	1.1	103
69	Hollow Cages versus Space-Filling Structures for Medium-Sized Gold Clusters:  The Spherical Aromaticity of the Au50 Cage. Journal of Physical Chemistry A, 2005, 109, 9265-9269.	1.1	101
70	Structure and structural evolution of () clusters using a genetic algorithm and density functional theory method. Solid State Communications, 2007, 144, 174-179.	0.9	101
71	N-doped graphitic carbon materials hybridized with transition metals (compounds) for hydrogen evolution reaction: Understanding the synergistic effect from atomistic level. Carbon, 2018, 133, 260-266.	5.4	100
72	Genetic Algorithms for the Geometry Optimization of Atomic and Molecular Clusters. Journal of Computational and Theoretical Nanoscience, 2004, 1, 117-131.	0.4	99

#	Article	IF	CITATIONS
73	Discovery of a silicon-based ferrimagnetic wheel structure in V _x Si ₁₂ ^{â^'} (x = 1–3) clusters: photoelectron spectroscopy and density functional theory investigation. Nanoscale, 2014, 6, 14617-14621.	2.8	99
74	Lateral heterostructures of monolayer group-IV monochalcogenides: band alignment and electronic properties. Journal of Materials Chemistry C, 2017, 5, 3788-3795.	2.7	94
75	A new phase diagram of water under negative pressure: The rise of the lowest-density clathrate s-III. Science Advances, 2016, 2, e1501010.	4.7	92
76	Band Gap Modulated by Electronic Superlattice in Blue Phosphorene. ACS Nano, 2018, 12, 5059-5065.	7.3	92
77	Stabilization of body-centred cubic iron under inner-core conditions. Nature Geoscience, 2017, 10, 312-316.	5.4	91
78	Growth behavior and magnetic properties ofSinFe(n=2–14)clusters. Physical Review B, 2006, 73, .	1.1	90
79	Inverse Capacity Growth and Pocket Effect in SnS ₂ Semifilled Carbon Nanotube Anode. ACS Nano, 2018, 12, 8037-8047.	7.3	90
80	Comprehensive genetic algorithm for <i>ab initio</i> global optimisation of clusters. Molecular Simulation, 2016, 42, 809-819.	0.9	88
81	Operando Revealing Dynamic Reconstruction of NiCo Carbonate Hydroxide for High-Rate Energy Storage. Joule, 2020, 4, 673-687.	11.7	88
82	Shuttle inhibition by chemical adsorption of lithium polysulfides in B and N co-doped graphene for Li–S batteries. Physical Chemistry Chemical Physics, 2016, 18, 25241-25248.	1.3	87
83	Accelerating polysulfide redox conversion on bifunctional electrocatalytic electrode for stable Li-S batteries. Energy Storage Materials, 2019, 20, 98-107.	9.5	87
84	Magnetic properties of atomic clusters and endohedral metallofullerenes. Coordination Chemistry Reviews, 2015, 289-290, 315-340.	9.5	86
85	Hybrids of PtRu Nanoclusters and Black Phosphorus Nanosheets for Highly Efficient Alkaline Hydrogen Evolution Reaction. ACS Catalysis, 2019, 9, 10870-10875.	5.5	86
86	Alloying effect on the elastic properties of refractory high-entropy alloys. Materials and Design, 2017, 114, 243-252.	3.3	85
87	Structural and vibrational properties of solid nitromethane under high pressure by density functional theory. Journal of Chemical Physics, 2006, 124, 124501.	1.2	82
88	Band alignment of two-dimensional lateral heterostructures. 2D Materials, 2017, 4, 015038.	2.0	80
89	Ni–Ta binary bulk metallic glasses. Scripta Materialia, 2010, 63, 178-180.	2.6	79
90	Eighteen functional monolayer metal oxides: wide bandgap semiconductors with superior oxidation resistance and ultrahigh carrier mobility. Nanoscale Horizons, 2019, 4, 592-600.	4.1	78

#	Article	IF	CITATIONS
91	Body-centered tetragonal B2N2: a novel sp3 bonding boron nitride polymorph. Physical Chemistry Chemical Physics, 2011, 13, 14565.	1.3	77
92	Energetics and electronic structures of AlN nanotubes/wires and their potential application as ammonia sensors. Nanotechnology, 2007, 18, 424023.	1.3	76
93	Intercalation and diffusion of lithium ions in a carbon nanotube bundle by ab initio molecular dynamics simulations. Energy and Environmental Science, 2011, 4, 1379.	15.6	76
94	Quantum transport properties of ultrathin silver nanowires. Nanotechnology, 2003, 14, 501-504.	1.3	75
95	Complete Spin Polarization for a Carbon Nanotube with an Adsorbed Atomic Transition-Metal Chain. Nano Letters, 2004, 4, 561-563.	4.5	75
96	A new class of epitaxial porphyrin metal–organic framework thin films with extremely high photocarrier generation efficiency: promising materials for all-solid-state solar cells. Journal of Materials Chemistry A, 2016, 4, 12739-12747.	5.2	75
97	Cooperative Electron–Phonon Coupling and Buckled Structure in Germanene on Au(111). ACS Nano, 2017, 11, 3553-3559.	7.3	75
98	Structures and electronic properties of symmetric and nonsymmetric graphene grain boundaries. Carbon, 2013, 55, 151-159.	5.4	74
99	MXene nanoribbons as electrocatalysts for the hydrogen evolution reaction with fast kinetics. Physical Chemistry Chemical Physics, 2018, 20, 19390-19397.	1.3	74
100	Tailorable AcceptorC60â^'nBnand DonorC60â^'mNmPairs for Molecular Electronics. Physical Review Letters, 2003, 90, 206602.	2.9	73
101	Atomic structures and covalent-to-metallic transition of lead clustersPbn(n=2–22). Physical Review A, 2005, 71, .	1.0	73
102	First-principles calculations of structural, electronic, vibrational, and magnetic properties of C60 and C48N12: A comparative study. Journal of Chemical Physics, 2003, 118, 8621-8635.	1.2	72
103	Stabilization of fullerene-like boron cages by transition metal encapsulation. Nanoscale, 2015, 7, 10482-10489.	2.8	72
104	Electronic and Photonic Properties of Doped Carbon Nanotubes. Journal of Nanoscience and Nanotechnology, 2003, 3, 459-478.	0.9	71
105	Engineering the Electronic Structure of Single-Walled Carbon Nanotubes by Chemical Functionalization. ChemPhysChem, 2005, 6, 598-601.	1.0	71
106	An exchange intercalation mechanism for the formation of a two-dimensional Si structure underneath graphene. Nano Research, 2012, 5, 352-360.	5.8	71
107	Graphene Oxide: Physics and Applications. SpringerBriefs in Physics, 2015, , .	0.2	70
108	GeAs and SiAs monolayers: Novel 2D semiconductors with suitable band structures. Physica E: Low-Dimensional Systems and Nanostructures, 2018, 95, 149-153.	1.3	70

#	Article	lF	CITATIONS
109	High-pressure behavior of crystalline FOX-7 by density functional theory calculations. Computational Materials Science, 2008, 42, 698-703.	1.4	69
110	Reverseâ€Graded 2D Ruddlesden–Popper Perovskites for Efficient Air‣table Solar Cells. Advanced Energy Materials, 2019, 9, 1900612.	10.2	69
111	A novel CuTi-containing catalyst derived from hydrotalcite-like compounds for selective catalytic reduction of NO with C3H6 under lean-burn conditions. Journal of Catalysis, 2014, 309, 268-279.	3.1	68
112	Atomic and Electronic Structures of Fluorinated BN Nanotubes:Â Computational Study. Journal of Physical Chemistry B, 2006, 110, 25678-25685.	1.2	67
113	Melting behavior of ultrathin titanium nanowires. Physical Review B, 2003, 67, .	1.1	66
114	2D lateral heterostructures of group-III monochalcogenide: Potential photovoltaic applications. Applied Physics Letters, 2018, 112, .	1.5	66
115	Boron fullerenes with 32–56 atoms: Irregular cage configurations and electronic properties. Chemical Physics Letters, 2010, 501, 16-19.	1.2	65
116	B ₂₈ : the smallest all-boron cage from an ab initio global search. Nanoscale, 2015, 7, 15086-15090.	2.8	65
117	The stability and electronic structure of single-walled ZnO nanotubes by density functional theory. Nanotechnology, 2007, 18, 345706.	1.3	64
118	Nonmetal-metal transition inZnn(n=2–20)clusters. Physical Review A, 2003, 68, .	1.0	63
119	Curved carbon nanotubes: From unique geometries to novel properties and peculiar applications. Nano Research, 2014, 7, 626-657.	5.8	63
120	Structures and Electronic Properties of V ₃ Si _{<i>n</i>} [–] (<i>n</i> =) Tj ET 10987-10994.	Qq0 0 0 r 1.5	gBT /Overloc 63
121	Structural and Electronic Properties of Interfaces in Graphene and Hexagonal Boron Nitride Lateral Heterostructures. Chemistry of Materials, 2016, 28, 5022-5028.	3.2	63
122	Structures and Magnetic Properties of MoS ₂ Grain Boundaries with Antisite Defects. Journal of Physical Chemistry C, 2017, 121, 12261-12269.	1.5	63
123	Two-dimensional ZnO for the selective photoreduction of CO ₂ . Journal of Materials Chemistry A, 2019, 7, 16294-16303.	5.2	62
124	Geometric and electronic properties of titanium clusters studied by ultrasoft pseudopotential. Solid State Communications, 2001, 118, 157-161.	0.9	61
125	Structure and electronic properties of cobalt atoms encapsulated in Sin (n=1–13) clusters. Chemical Physics Letters, 2005, 411, 279-284.	1.2	61
126	Distinct properties of single-wall carbon nanotubes with monovalent sidewall additions. Nanotechnology, 2005, 16, 635-638.	1.3	61

#	Article	IF	CITATIONS
127	First-principles studies of diamond polytypes. Diamond and Related Materials, 2008, 17, 356-364.	1.8	61
128	Accurate electronic properties and non-linear optical response of two-dimensional MA2Z4. Nanoscale, 2021, 13, 5479-5488.	2.8	61
129	Cage and tube structures of medium-sized zinc oxide clusters (ZnO)n (n=24, 28, 36, and 48). Journal of Chemical Physics, 2008, 128, 144710.	1.2	60
130	Two-Dimensional Metallic NiTe ₂ with Ultrahigh Environmental Stability, Conductivity, and Electrocatalytic Activity. ACS Nano, 2020, 14, 9011-9020.	7.3	60
131	Tunable Assembly of sp ³ Cross‣inked 3D Graphene Monoliths: A Firstâ€Principles Prediction. Advanced Functional Materials, 2013, 23, 5846-5853.	7.8	59
132	Excellent HER and OER Catalyzing Performance of Seâ€Vacancies in Defectsâ€Engineered PtSe ₂ : From Simulation to Experiment. Advanced Energy Materials, 2022, 12, 2102359.	10.2	59
133	Direct synthesis and in situ characterization of monolayer parallelogrammic rhenium diselenide on gold foil. Communications Chemistry, 2018, 1, .	2.0	58
134	Monolayer group-III monochalcogenides by oxygen functionalization: a promising class of two-dimensional topological insulators. Npj Quantum Materials, 2018, 3, .	1.8	58
135	Structure and stability of bilayer borophene: The roles of hexagonal holes and interlayer bonding. FlatChem, 2018, 7, 48-54.	2.8	58
136	Immobilized trimeric metal clusters: A family of the smallest catalysts for selective CO2 reduction toward multi-carbon products. Nano Energy, 2020, 76, 105049.	8.2	56
137	Effect of surface Lewis acidity on selective catalytic reduction of NO by C3H6 over calcined hydrotalcite. Applied Catalysis A: General, 2013, 451, 176-183.	2.2	55
138	Controllable Conversion of CO ₂ on Nonâ€Metallic Gold Clusters. Angewandte Chemie - International Edition, 2020, 59, 1919-1924.	7.2	55
139	Structures and electronic properties of ultrathin titanium nanowires. Journal of Physics Condensed Matter, 2001, 13, L403-L408.	0.7	53
140	Structure and magnetic properties of cobalt doped () clusters. Physics Letters, Section A: General, Atomic and Solid State Physics, 2007, 367, 335-344.	0.9	53
141	Phosphorus quantum dots as visible-light photocatalyst for water splitting. Computational Materials Science, 2017, 130, 56-63.	1.4	53
142	Atomic Sulfur Anchored on Silicene, Phosphorene, and Borophene for Excellent Cycle Performance of Li–S Batteries. ACS Applied Materials & Interfaces, 2017, 9, 42836-42844.	4.0	53
143	Structure and magnetic properties of Co-Cu bimetallic clusters. Physical Review B, 2002, 66, .	1.1	52
144	Functionalization of BN nanotubes with dichlorocarbenes. Nanotechnology, 2008, 19, 015202.	1.3	52

#	Article	IF	CITATIONS
145	Titanium-decorated graphene oxide for carbon monoxide capture and separation. Physical Chemistry Chemical Physics, 2011, 13, 21126.	1.3	52
146	Mechanical and electronic properties of B ₁₂ -based ternary crystals of orthorhombic phase. Journal of Physics Condensed Matter, 2010, 22, 315503.	0.7	51
147	Stability and dissolution of helium–vacancy complexes in vanadium solid. Journal of Nuclear Materials, 2011, 419, 1-8.	1.3	51
148	A Molecularâ€Cage Strategy Enabling Efficient Chemisorption–Electrocatalytic Interface in Nanostructured Li ₂ S Cathode for Li Metalâ€Free Rechargeable Cells with High Energy. Advanced Functional Materials, 2019, 29, 1905986.	7.8	51
149	Copper(<scp>i</scp>) sulfide: a two-dimensional semiconductor with superior oxidation resistance and high carrier mobility. Nanoscale Horizons, 2019, 4, 223-230.	4.1	51
150	Pressure-induced metallization in solid boron. Physical Review B, 2002, 66, .	1.1	50
151	Firstâ€principles study of molecular hydrogen dissociation on doped Al ₁₂ X (X = B, Al, C, Si,) Tj ETQq	1 1 0.7843 1.5	314 rgBT /0
152	Atomic structures and electronic properties of phosphorene grain boundaries. 2D Materials, 2016, 3, 025008.	2.0	49
153	Structures, electronic properties, and hydrogen-storage capacity of single-walled TiO2 nanotubes. Physica E: Low-Dimensional Systems and Nanostructures, 2009, 41, 838-842.	1.3	48
154	He-induced vacancy formation in bcc Fe solid from first-principles simulation. Journal of Nuclear Materials, 2014, 444, 147-152.	1.3	48
155	Initial Growth Mechanism of Blue Phosphorene on Au(111) Surface. Journal of Physical Chemistry C, 2017, 121, 17893-17899.	1.5	48
156	Characteristics of Raman spectra for graphene oxide from <i>ab initio</i> simulations. Journal of Chemical Physics, 2011, 135, 184503.	1.2	47
157	Boron clusters with 46, 48, and 50 atoms: competition among the core–shell, bilayer and quasi-planar structures. Nanoscale, 2017, 9, 13905-13909.	2.8	47
158	Structural transition of Si clusters and their thermodynamics. Chemical Physics Letters, 2001, 341, 529-534.	1.2	46
159	Vibrational properties of molecule and crystal of TATB: A comparative density functional study. Physics Letters, Section A: General, Atomic and Solid State Physics, 2006, 358, 63-69.	0.9	46
160	Transformation from chemisorption to physisorption with tube diameter and gas concentration: Computational studies on NH3 adsorption in BN nanotubes. Journal of Chemical Physics, 2007, 127, 184705.	1.2	46
161	Improving hydrogen storage properties of covalent organic frameworks by substitutional doping. International Journal of Hydrogen Energy, 2010, 35, 266-271.	3.8	46
162	What is the best density functional to describe water clusters: evaluation of widely used density functionals with various basis sets for (H2O) n (nÂ=Â1–10). Theoretical Chemistry Accounts, 2011, 130, 341-352.	0.5	46

#	Article	IF	CITATIONS
163	Computational high-throughput screening of alloy nanoclusters for electrocatalytic hydrogen evolution. Npj Computational Materials, 2021, 7, .	3.5	46
164	Structural, electronic, and magnetic properties of heterofullerene C48B12. Chemical Physics Letters, 2003, 375, 445-451.	1.2	45
165	True Nanocable Assemblies with Insulating BN Nanotube Sheaths and Conducting Cu Nanowire Cores. Journal of Physical Chemistry B, 2006, 110, 2529-2532.	1.2	45
166	Structure and electronic properties of medium-sized GanNn clusters (n=4–12). Chemical Physics Letters, 2006, 422, 170-173.	1.2	45
167	First-Principles Study of Water Chains Encapsulated in Single-Walled Carbon Nanotube. Journal of Physical Chemistry C, 2009, 113, 5368-5375.	1.5	45
168	Atomic structures and electronic properties of small Au–Ag binary clusters: Effects of size and composition. Computational and Theoretical Chemistry, 2012, 993, 36-44.	1.1	45
169	Combining Machine Learning Potential and Structure Prediction for Accelerated Materials Design and Discovery. Journal of Physical Chemistry Letters, 2020, 11, 8710-8720.	2.1	45
170	Elastic properties of vanadium-based alloys from first-principles theory. Physical Review B, 2012, 86, .	1.1	44
171	Crystal-Phase-Mediated Restructuring of Pt on TiO ₂ with Tunable Reactivity: Redispersion versus Reshaping. ACS Catalysis, 2022, 12, 3634-3643.	5.5	44
172	Dual Relationship between Large Gold Clusters (Antifullerenes) and Carbon Fullerenes:  A New Lowest-Energy Cage Structure for Au50. Journal of Physical Chemistry A, 2007, 111, 411-414.	1.1	43
173	High-pressure behavior of TATB crystal by density functional theory. Physics Letters, Section A: General, Atomic and Solid State Physics, 2007, 367, 383-388.	0.9	43
174	Atomic Structure of the Magic (ZnO) ₆₀ Cluster: First-Principles Prediction of a Sodalite Motif for ZnO Nanoclusters. Journal of Physical Chemistry C, 2010, 114, 5741-5744.	1.5	43
175	<i>Ab initio</i> molecular dynamics simulation of binary Cu64Zr36 bulk metallic glass: Validation of the cluster-plus-glue-atom model. Journal of Applied Physics, 2011, 109, .	1.1	43
176	A novel superhard BN allotrope under cold compression of h-BN. Journal of Physics Condensed Matter, 2013, 25, 122204.	0.7	43
177	Stacking fault energy of face-centered cubic metals: thermodynamic and <i>ab initio</i> approaches. Journal of Physics Condensed Matter, 2016, 28, 395001.	0.7	43
178	Hydrogen storage properties of destabilized MgH2–Li3AlH6 system. International Journal of Hydrogen Energy, 2010, 35, 8122-8129.	3.8	42
179	First-principle study of the structural, electronic, and magnetic properties of amorphous Fe–B alloys. Physica B: Condensed Matter, 2012, 407, 250-257.	1.3	42
180	Hexagonal M ₂ C ₃ (M = As, Sb, and Bi) monolayers: new functional materials with desirable band gaps and ultrahigh carrier mobility. Journal of Materials Chemistry C, 2018, 6, 12689-12697.	2.7	42

#	Article	IF	CITATIONS
181	Optical properties and photonic devices of doped carbon nanotubes. Analytica Chimica Acta, 2006, 568, 161-170.	2.6	41
182	First-principles study of pentaerythritol tetranitrate single crystals under high pressure: Vibrational properties. Chemical Physics Letters, 2006, 428, 394-399.	1.2	41
183	First-principle studies of Al–Ru intermetallic compounds. Intermetallics, 2008, 16, 333-339.	1.8	41
184	Point defects in group III nitrides: A comparative first-principles study. Journal of Applied Physics, 2019, 125, .	1.1	41
185	Excitonic Au ₄ Ru ₂ (PPh ₃) ₂ (SC ₂ H ₄ Ph) _{ cluster for light-driven dinitrogen fixation. Chemical Science, 2020, 11, 2440-2447.}	8< ≉sı zıb>	41
186	Low-dimensional non-metal catalysts: principles for regulating p-orbital-dominated reactivity. Npj Computational Materials, 2021, 7, .	3.5	41
187	Storage Capacity and Vibration Frequencies of Guest Molecules in CH ₄ and CO ₂ Hydrates by First-Principles Calculations. Journal of Physical Chemistry A, 2014, 118, 215-222.	1.1	40
188	Ab initio-predicted micro-mechanical performance of refractory high-entropy alloys. Scientific Reports, 2015, 5, 12334.	1.6	40
189	Electronic Structures of Germanene on MoS ₂ : Effect of Substrate and Molecular Adsorption. Journal of Physical Chemistry C, 2016, 120, 21691-21698.	1.5	40
190	Superconductivity in two-dimensional phosphorus carbide (β ₀ -PC). Physical Chemistry Chemical Physics, 2018, 20, 12362-12367.	1.3	40
191	Scalable Production of Freestanding Few-Layer β ₁₂ -Borophene Single Crystalline Sheets as Efficient Electrocatalysts for Lithium–Sulfur Batteries. ACS Nano, 2021, 15, 17327-17336.	7.3	40
192	Density functional study of beryllium clusters, with gradient correction. Journal of Physics Condensed Matter, 2001, 13, L753-L758.	0.7	39
193	Dipole polarizabilities of germanium clusters. Chemical Physics Letters, 2003, 367, 448-454.	1.2	39
194	Competition Among fcc-Like, Double-Layered Flat, Tubular Cage, and Close-Packed Structural Motifs for Medium-Sized Aun (n = 21â^'28) Clusters. Journal of Physical Chemistry A, 2008, 112, 3141-3144.	1.1	39
195	Structural, mechanical, and electronic properties of ultrathin ZnO nanowires. Applied Physics Letters, 2008, 93, 021918.	1.5	39
196	First-principles study of Ru atoms and clusters adsorbed outside and inside carbon nanotubes. Journal of Chemical Physics, 2010, 132, 234704.	1.2	39
197	Strength and fracture behavior of graphene grain boundaries: effects of temperature, inflection, and symmetry from molecular dynamics. Physical Chemistry Chemical Physics, 2013, 15, 11794.	1.3	39
198	Magic structures of helical multishell zirconium nanowires. Physical Review B, 2002, 65, .	1.1	38

#	Article	IF	CITATIONS
199	Tunable optical properties of icosahedral, dodecahedral, and tetrahedral clusters. Physical Review B, 2005, 71, .	1.1	38
200	Formation of stable fullerenelikeGanAsnclusters(6≤â‰9): Gradient-corrected density-functional theory and a genetic global optimization approach. Physical Review B, 2006, 74, .	1.1	38
201	Stability and migration property of helium and self defects in vanadium and V–4Cr–4Ti alloy by first-principles. Journal of Nuclear Materials, 2011, 413, 90-94.	1.3	38
202	Dissociation mechanism of carbon dioxide hydrate by molecular dynamic simulation and ab initio calculation. Computational and Theoretical Chemistry, 2012, 991, 165-173.	1.1	38
203	Unique Transformation from Graphene to Carbide on Re(0001) Induced by Strong Carbon–Metal Interaction. Journal of the American Chemical Society, 2017, 139, 17574-17581.	6.6	38
204	Two-dimensional spin–valley-coupled Dirac semimetals in functionalized SbAs monolayers. Materials Horizons, 2019, 6, 781-787.	6.4	38
205	Controlling the synthesis of uniform electron-deficient Pd clusters for superior hydrogen production from formic acid. Journal of Materials Chemistry A, 2019, 7, 10363-10371.	5.2	38
206	Density-functional study of structures and electronic properties of Cd clusters. Physical Review A, 2001, 64, .	1.0	37
207	Growth control, interface behavior, band alignment, and potential device applications of 2D lateral heterostructures. Wiley Interdisciplinary Reviews: Computational Molecular Science, 2018, 8, e1353.	6.2	37
208	Selective Câ^'C Coupling by Spatially Confined Dimeric Metal Centers. IScience, 2020, 23, 101051.	1.9	37
209	Semiconducting allotrope of graphene. Nanotechnology, 2012, 23, 385704.	1.3	36
210	Solid–Solution Semiconductor Nanowires in Pseudobinary Systems. Nano Letters, 2013, 13, 85-90.	4.5	36
211	Prediction of a new ice clathrate with record low density: A potential candidate as ice XIX in guest-free form. Chemical Physics Letters, 2017, 671, 186-191.	1.2	36
212	New metallic carbon: Three dimensionally carbon allotropes comprising ultrathin diamond nanostripes. Carbon, 2018, 126, 601-610.	5.4	36
213	Point defects in epitaxial silicene on Ag(111) surfaces. 2D Materials, 2016, 3, 025034.	2.0	35
214	Giant magnetic anisotropy of a 5d transition metal decorated two-dimensional polyphthalocyanine framework. Journal of Materials Chemistry C, 2016, 4, 2147-2154.	2.7	35
215	Defects and oxidation of group-III monochalcogenide monolayers. Journal of Chemical Physics, 2017, 147, 104709.	1.2	35
216	Mass spectrometric and first principles study of AlnCâ^' clusters. Solid State Communications, 2002, 122, 543-547.	0.9	34

#	Article	IF	CITATIONS
217	Reduced Li diffusion barriers in composite BC3 nanotubes. Chemical Physics Letters, 2005, 415, 323-326.	1.2	34
218	Structural growth behavior and polarizability of CdnTenâ€^(n=1–14) clusters. Journal of Chemical Physics, 2009, 130, 214307.	1.2	34
219	Electronic and transport gaps of graphene opened by grain boundaries. Journal of Applied Physics, 2012, 112, .	1.1	34
220	Retention and diffusion of H, He, O, C impurities in Be. Journal of Nuclear Materials, 2012, 423, 164-169.	1.3	34
221	Trapping of multiple hydrogen atoms in a vanadium monovacancy: A first-principles study. Journal of Nuclear Materials, 2012, 429, 216-220.	1.3	34
222	Mechanical properties of bilayer graphene with twist and grain boundaries. Journal of Applied Physics, 2013, 113, .	1.1	34
223	Low-Energy Structures of Binary Pt–Sn Clusters from Global Search Using Genetic Algorithm and Density Functional Theory. Journal of Cluster Science, 2015, 26, 389-409.	1.7	34
224	Selecting electrode materials for monolayer ReS ₂ with an Ohmic contact. Journal of Materials Chemistry C, 2018, 6, 6764-6770.	2.7	34
225	Al–Mg–B thin films prepared by magnetron sputtering. Vacuum, 2010, 85, 541-545.	1.6	33
226	Lowest-energy structures and electronic properties of Na-Si binary clusters from <i>ab initio</i> global search. Journal of Chemical Physics, 2011, 135, 184305.	1.2	33
227	Study on interactions between Cadmium and defects in Cd-doped ZnO by first-principle calculations. Solid State Sciences, 2011, 13, 384-387.	1.5	33
228	First-principles study of the behavior of O, N and C impurities in vanadium solids. Journal of Nuclear Materials, 2013, 435, 71-76.	1.3	33
229	Elastic constants of random solid solutions by SQS and CPA approaches: the case of fcc Ti-Al. Journal of Physics Condensed Matter, 2015, 27, 315702.	0.7	33
230	Oxygen Evolution Reaction over the Au/YSZ Interface at High Temperature. Angewandte Chemie - International Edition, 2019, 58, 4617-4621.	7.2	33
231	Thermal properties of medium-sized Ge clusters. Solid State Communications, 2001, 117, 593-598.	0.9	32
232	Optimally stuffed fullerene structures of silicon nanoclusters. Physical Review B, 2005, 71, .	1.1	32
233	Structural evolution of medium-sized Pdnâ€^(n=15–25) clusters from density functional theory. Journal of Chemical Physics, 2008, 129, 114302.	1.2	32
234	First-principles study of transition metal doped Li2S as cathode materials in lithium batteries. Journal of Renewable and Sustainable Energy, 2012, 4, .	0.8	32

#	Article	IF	CITATIONS
235	Vacancy trapping mechanism for multiple helium in monovacancy and small void of vanadium solid. Journal of Nuclear Materials, 2013, 440, 557-561.	1.3	32
236	Two-dimensional intrinsic ferromagnets with high Curie temperatures: synthesis, physical properties and device applications. Journal of Materials Chemistry C, 2021, 9, 6103-6121.	2.7	32
237	Thermal behavior of Cu–Co bimetallic clusters. Solid State Communications, 2001, 119, 13-18.	0.9	31
238	Exceptional Electrochemical HER Performance with Enhanced Electron Transfer between Ru Nanoparticles and Single Atoms Dispersed on a Carbon Substrate. Angewandte Chemie, 2021, 133, 16180-16186.	1.6	31
239	MXene and MBene as efficient catalysts for energy conversion: roles of surface, edge and interface. JPhys Energy, 2021, 3, 012002.	2.3	31
240	Genetic-algorithm prediction of the magic-number structure of(C60)Nclusters with a first-principles interaction potential. Physical Review B, 1999, 59, 14903-14906.	1.1	30
241	The R3-carbon allotrope: a pathway towards glassy carbon under high pressure. Scientific Reports, 2013, 3, 1877.	1.6	30
242	Band gap opening in bilayer silicene by alkali metal intercalation. Journal of Physics Condensed Matter, 2014, 26, 475303.	0.7	30
243	Mo Concentration Controls the Morphological Transitions from Dendritic to Semicompact, and to Compact Growth of Monolayer Crystalline MoS2 on Various Substrates. ACS Applied Materials & Interfaces, 2019, 11, 42751-42759.	4.0	30
244	Critical size for a metal-nonmetal transition in transition-metal clusters. Physical Review B, 1994, 50, 15424-15426.	1.1	29
245	First-principles study of hydrogen in perfect tungsten crystal. Nuclear Instruments & Methods in Physics Research B, 2009, 267, 3170-3174.	0.6	29
246	Lowest-energy structures of (MgO)n (n=2–7) clusters from a topological method and first-principles calculations. Computational and Theoretical Chemistry, 2012, 980, 62-67.	1.1	29
247	Structure, Electrode Voltage and Activation Energy of LiMn _x Co _y Ni _{1-x-y} O ₂ Solid Solutions as Cathode Materials for Li Batteries from First-Principles. Journal of the Electrochemical Society, 2012, 159, A1203-A1208.	1.3	29
248	Reaction mechanisms of graphene oxide chemical reduction by sulfur-containing compounds. Carbon, 2014, 67, 146-155.	5.4	29
249	The effect of size distributions of Si nanoclusters on photoluminescence from ensembles of Si nanoclusters. Physics Letters, Section A: General, Atomic and Solid State Physics, 1996, 212, 285-289.	0.9	28
250	A transferable nonorthogonal tight-binding model of germanium: application to small clusters. Physics Letters, Section A: General, Atomic and Solid State Physics, 2000, 275, 281-286.	0.9	28
251	Cluster-assembled materials based onNa6Pb. Physical Review B, 2003, 68, .	1.1	28
252	Density-functional study of small and medium-sizedAsnclusters up ton=28. Physical Review B, 2006, 73,	1,1	28

#	Article	IF	CITATIONS
253	Water Clusters Confined in Nonpolar Cavities by Ab Initio Calculations. Journal of Physical Chemistry C, 2008, 112, 11779-11785.	1.5	28
254	Stability and magnetic properties of transition metal atoms endohedral BnNnâ€^(n=12–28) cages. Journal of Chemical Physics, 2008, 128, 084306.	1.2	28
255	Mechanisms of H2 generation for metal doped Al16M (MÂ=ÂMg and Bi) clusters in water. International Journal of Hydrogen Energy, 2013, 38, 6930-6937.	3.8	28
256	Engineering magnetic anisotropy in two-dimensional magnetic materials. Advances in Physics: X, 2018, 3, 1432415.	1.5	28
257	Defect stability and electronic structure of doped β-Ga2O3: A comprehensive ab initio study. Journal of Alloys and Compounds, 2019, 794, 374-384.	2.8	28
258	Silicene catalysts for CO ₂ hydrogenation: the number of layers controls selectivity. Nanoscale, 2019, 11, 7734-7743.	2.8	28
259	Wavelength-Tunable Optical Fiber Localized Surface Plasmon Resonance Biosensor <i>via</i> a Diblock Copolymer-Templated Nanorod Monolayer. ACS Applied Materials & Interfaces, 2020, 12, 50929-50940.	4.0	28
260	Tuning the electronic properties of bilayer black phosphorene with the twist angle. Journal of Materials Chemistry C, 2020, 8, 6264-6272.	2.7	28
261	Ultrahigh hydrogen storage capacity of holey graphyne. Nanotechnology, 2021, 32, 215402.	1.3	28
262	Superatomic Signature and Reactivity of Silver Clusters with Oxygen: Double Magic Ag ₁₇ [–] with Geometric and Electronic Shell Closure. CCS Chemistry, 2021, 3, 219-229.	4.6	28
263	Structural, Electronic, and Magnetic Properties of Small Vanadium Clusters. Physica Status Solidi (B): Basic Research, 1999, 215, 1127-1135.	0.7	27
264	First-principles intermolecular binding energies in organic molecular crystals. Chemical Physics Letters, 2004, 388, 175-180.	1.2	27
265	Structural and electronic properties ofSbn(n=2–10)clusters using density-functional theory. Physical Review A, 2005, 72, .	1.0	27
266	Structures and quantum conductances of atomic-sized copper nanowires. Nanotechnology, 2006, 17, 3178-3182.	1.3	27
267	Lowest-energy structures of AlnPn (n=1–9) clusters from density functional theory. Chemical Physics Letters, 2007, 443, 29-33.	1.2	27
268	Effect of B/C ratio on the physical properties of highly boron-doped diamond films. Vacuum, 2010, 84, 930-934.	1.6	27
269	Electronic and magnetic properties for Co13 clusters deposited on graphene: A first-principles exploration. Physica E: Low-Dimensional Systems and Nanostructures, 2012, 46, 6-11.	1.3	27
270	Graphene oxide and lithium amidoborane: a new way to bridge chemical and physical approaches for hydrogen storage. Journal of Materials Chemistry A, 2013, 1, 8016.	5.2	27

#	Article	IF	CITATIONS
271	Strong Adlayer–Substrate Interactions "Break―the Patching Growth of <i>h</i> -BN onto Graphene on Re(0001). ACS Nano, 2017, 11, 1807-1815.	7.3	27
272	Structures and electronic properties of B3Sinâ^' (n = 4–10) clusters: A combined <i>ab initio</i> and experimental study. Journal of Chemical Physics, 2017, 146, 044306.	1.2	27
273	Which Density Functional Should Be Used to Describe Protonated Water Clusters?. Journal of Physical Chemistry A, 2017, 121, 3117-3127.	1.1	27
274	Vanadium carbide coating as hydrogen permeation barrier: A DFT study. International Journal of Hydrogen Energy, 2019, 44, 6093-6102.	3.8	27
275	Optical excitation and absorption spectra of C50Cl10. Journal of Chemical Physics, 2004, 121, 2849-2851.	1.2	26
276	Density-functional study of structural and electronic properties ofAlnN(n=2–12)clusters. Physical Review A, 2005, 72, .	1.0	26
277	The isolable matryoshka nesting doll icosahedral cluster [As@Ni12@As20]3â^'as a "superatom†analogy with the jellium cluster Al13â^'generated in the gas phase by laser vaporization. Chemical Communications, 2006, , 4204-4205.	2.2	26
278	Mechanical and thermal properties of methane clathrate hydrates as an alternative energy resource. Journal of Renewable and Sustainable Energy, 2011, 3, 063110.	0.8	26
279	Nonstandard cages in the formation process of methane clathrate: Stability, structure, and spectroscopic implications from first-principles. Journal of Chemical Physics, 2012, 136, 224508.	1.2	26
280	Halogen-doping in LiCoO ₂ cathode materials for Li-ion batteries: insights from ab initio calculations. RSC Advances, 2015, 5, 107326-107332.	1.7	26
281	Electrode potential and activation energy of sodium transition-metal oxides as cathode materials for sodium batteries: A first-principles investigation. Computational Materials Science, 2015, 106, 15-22.	1.4	26
282	He–vacancy interaction and multiple He trapping in small void of silicon carbide. Journal of Nuclear Materials, 2015, 457, 36-41.	1.3	26
283	Tunable Thermal Conductivity of Silicene by Germanium Doping. Journal of Superconductivity and Novel Magnetism, 2016, 29, 717-720.	0.8	26
284	Long life rechargeable Li-O2 batteries enabled by enhanced charge transfer in nanocable-like Fe@N-doped carbon nanotube catalyst. Science China Materials, 2017, 60, 415-426.	3.5	26
285	Energetics of helium-vacancy complexes in Fe-9Cr alloys from first-principles calculations. Journal of Nuclear Materials, 2019, 513, 143-151.	1.3	26
286	Optimization of photocarrier dynamics and activity in phosphorene with intrinsic defects for nitrogen fixation. Journal of Materials Chemistry A, 2020, 8, 20570-20580.	5.2	26
287	A simple d-band model for the magnetic property of ferromagnetic transition-metal clusters. Physics Letters, Section A: General, Atomic and Solid State Physics, 1995, 205, 308-312.	0.9	25
288	n-diamond: an intermediate state between rhombohedral graphite and diamond?. New Journal of Physics, 2006, 8, 62-62.	1.2	25

#	Article	IF	CITATIONS
289	Lowest-energy structures of (WO3)n (2≤≽2) clusters from first-principles global search. Chemical Physics Letters, 2012, 544, 7-12.	1.2	25
290	He–He and He–metal interactions in transition metals from first-principles. Journal of Nuclear Materials, 2015, 467, 465-471.	1.3	25
291	2D lateral heterostructures of monolayer and bilayer phosphorene. Journal of Materials Chemistry C, 2017, 5, 2291-2300.	2.7	25
292	Interaction between helium and intrinsic point defects in 3C-SiC single crystal. Journal of Applied Physics, 2017, 121, .	1.1	25
293	Identifying the Non-Identical Outermost Selenium Atoms and Invariable Band Gaps across the Grain Boundary of Anisotropic Rhenium Diselenide. ACS Nano, 2018, 12, 10095-10103.	7.3	25
294	Realization of Strained Stanene by Interface Engineering. Journal of Physical Chemistry Letters, 2019, 10, 1558-1565.	2.1	25
295	Enhanced Ferromagnetism of Crl ₃ Bilayer by Self-Intercalation*. Chinese Physics Letters, 2020, 37, 107506.	1.3	25
296	Electromagnetic wave absorption properties of carbon powder from catalysed carbon black in X and Ku bands. Journal Physics D: Applied Physics, 2006, 39, 1960-1962.	1.3	24
297	Nanocables made of a transition metal wire and boron nitride sheath: Density functional calculations. Physical Review B, 2006, 74, .	1.1	24
298	Elastic properties of hydrous forsterites under high pressure: First-principle calculations. Physics of the Earth and Planetary Interiors, 2009, 176, 89-97.	0.7	24
299	Lowest-energy structures of cationic <mml:math <br="" xmlns:mml="http://www.w3.org/1998/Math/MathML">altimg="si1.gif" display="inline" overflow="scroll"><mml:mrow><mml:msubsup><mml:mrow><mml:mtext>P</mml:mtext></mml:mrow><mml:mr (m= 1â€"12) clusters from first-principles simulated annealing. Chemical Physics Letters, 2010, 485, 26-30.</mml:mr </mml:msubsup></mml:mrow></mml:math>	1.2 o₩> <mml< td=""><td>:mn>2</td></mml<>	:mn>2
300	Ab initio molecular dynamics simulation of binary Ni62.5Nb37.5 bulk metallic glass: validation of the cluster-plus-glue-atom model. Journal of Materials Science, 2012, 47, 7628-7634.	1.7	24
301	Possible Formation of Graphyne on Transition Metal Surfaces: A Competition with Graphene from the Chemical Potential Point of View. Journal of Physical Chemistry C, 2016, 120, 14699-14705.	1.5	24
302	Reactions of Copper and Silver Cations with Carbon Dioxide: An Infrared Photodissociation Spectroscopic and Theoretical Study. Journal of Physical Chemistry A, 2017, 121, 3220-3226.	1.1	24
303	Hydrated Sodium Ion Clusters [Na+(H2O)n (n = 1–6)]: An ab initio Study on Structures and Non-covalent Interaction. Frontiers in Chemistry, 2019, 7, 624.	1.8	24
304	All-Silicon Topological Semimetals with Closed Nodal Line. Journal of Physical Chemistry Letters, 2019, 10, 244-250.	2.1	24
305	High-Curie-temperature ferromagnetism in bilayer <mml:math xmlns:mml="http://www.w3.org/1998/Math/MathML"><mml:mrow><mml:mi>Cr</mml:mi><mml:msub><mml:mi mathvariant="normal">I<mml:mn>3</mml:mn></mml:mi </mml:msub></mml:mrow> on bulk semiconducting substrates. Physical Review Materials. 2020. 4.</mml:math 	0.9	24
306	Lowest-energy endohedral fullerene structures of SiN(30⩽N⩽39)clusters by density functional calculations. Physical Review A, 2006, 73, .	1.0	23

#	Article	IF	CITATIONS
307	Magnetic properties of transition-metal impurities in silicon quantum dots. Physical Review B, 2007, 75,	1.1	23
308	Anisotropy in stability and Young's modulus of hydrogenated silicon nanowires. Chemical Physics Letters, 2008, 452, 183-187.	1.2	23
309	Structural growth sequences and electronic properties of manganese-doped germanium clusters: MnGe _{<i>n</i>} (2–15). Journal of Physics Condensed Matter, 2008, 20, 335223.	0.7	23
310	Design of Three-shell Icosahedral Matryoshka Clusters A@B12@A20 (A = Sn, Pb; B = Mg, Zn, Cd, Mn). Scientific Reports, 2014, 4, 6915.	1.6	23
311	Two-dimensional B–C–O alloys: a promising class of 2D materials for electronic devices. Nanoscale, 2016, 8, 8910-8918.	2.8	23
312	Schottky barrier at graphene/metal oxide interfaces: insight from first-principles calculations. Scientific Reports, 2017, 7, 41771.	1.6	23
313	Structural Evolution and Superatoms in Molybdenum Atom Stabilized Boron Clusters: MoBn (n = 10–24). Journal of Cluster Science, 2018, 29, 847-852.	1.7	23
314	Two-Dimensional AXenes: A New Family of Room-Temperature d ⁰ Ferromagnets and Their Structural Phase Transitions. Journal of Physical Chemistry Letters, 2019, 10, 7753-7759.	2.1	23
315	Efficient Photoexcited Charge Separation at the Interface of a Novel 0D/2D Heterojunction: A Time-Dependent Ultrafast Dynamic Study. Journal of Physical Chemistry Letters, 2021, 12, 2312-2319.	2.1	23
316	Tight-binding study of the structural and magnetic properties of vanadium clusters. Physica B: Condensed Matter, 1995, 215, 377-382.	1.3	22
317	Competition between supercluster and stuffed cage structures in medium-sized Gen (n=30–39) clusters. Journal of Chemical Physics, 2008, 128, 024302.	1.2	22
318	Electronic and magnetic properties of manganese and iron-doped GanAsn nanocages (n=7–12). Journal of Chemical Physics, 2008, 129, 044908.	1.2	22
319	What is atomic structures of (ZnO)34 magic cluster?. Physics Letters, Section A: General, Atomic and Solid State Physics, 2010, 374, 850-853.	0.9	22
320	First-principles studies on the thermal decomposition behavior of FOX-7. High Pressure Research, 2010, 30, 301-309.	0.4	22
321	Mechanical properties and defective effects of bcc V–4Cr–4Ti and V–5Cr–5Ti alloys by first-principles simulations. Computational Materials Science, 2011, 50, 2727-2731.	1.4	22
322	Structure, energetics, and heteroatom doping of armchair carbon nanotori. Carbon, 2011, 49, 4518-4523.	5.4	22
323	First-principles study of hydrogen behavior in V–Cr–Ti alloys. Nuclear Instruments & Methods in Physics Research B, 2011, 269, 1735-1739.	0.6	22
324	Structures and lattice energies of molecular crystals using density functional theory: Assessment of a local atomic potential approach. Chemical Physics Letters, 2012, 550, 94-98.	1.2	22

#	Article	IF	CITATIONS
325	Ideal strength of random alloys from first principles. Physical Review B, 2013, 87, .	1.1	22
326	An amorphous SiO2/4H-SiC(0001) interface: Band offsets and accurate charge transition levels of typical defects. Solid State Communications, 2015, 205, 28-32.	0.9	22
327	Chemically Engineering Magnetic Anisotropy of 2D Metalloporphyrin. Advanced Science, 2017, 4, 1700019.	5.6	22
328	Coordination-induced CO ₂ fixation into carbonate by metal oxides. Physical Chemistry Chemical Physics, 2018, 20, 19314-19320.	1.3	22
329	Anionic Copper Clusters Reacting with NO: An Open-Shell Superatom Cu ₁₈ [–] . Journal of Physical Chemistry Letters, 2020, 11, 5807-5814.	2.1	22
330	First-Principles Study of the Atomic Structures and Catalytic Properties of Monolayer TaS ₂ with Intrinsic Defects. Journal of Physical Chemistry C, 2021, 125, 10362-10369.	1.5	22
331	Fractional bond model for silicon clusters. Physical Review B, 1999, 60, 10703-10706.	1.1	21
332	Relative stability of hydrogenated nanodiamond and nanographite from density function theory. Chemical Physics Letters, 2007, 441, 318-321.	1.2	21
333	Structural transitions and electronic properties of the ultrathin SiC nanotubes under uniaxial compression. Chemical Physics Letters, 2008, 461, 280-284.	1.2	21
334	Mechanical and electronic properties of diamond nanowires under tensile strain from first principles. Nanotechnology, 2011, 22, 405705.	1.3	21
335	Stability and migration of vacancy in V–4Cr–4Ti alloy: Effects of Al, Si, Y trace elements. Journal of Nuclear Materials, 2013, 442, 370-376.	1.3	21
336	A Ternary Alloy Substrate to Synthesize Monolayer Graphene with Liquid Carbon Precursor. ACS Nano, 2017, 11, 1371-1379.	7.3	21
337	Interaction between Post-Graphene Group-IV Honeycomb Monolayers and Metal Substrates: Implication for Synthesis and Structure Control. Journal of Physical Chemistry C, 2017, 121, 5123-5129.	1.5	21
338	CPA descriptions of random Cu-Au alloys in comparison with SQS approach. Computational Materials Science, 2017, 128, 302-309.	1.4	21
339	xmlns:mml="http://www.w3.org/1998/Math/MathML"> <mml:mrow><mml:mi mathvariant="normal">N<mml:msub><mml:mi mathvariant="normal">H<mml:mn>3</mml:mn></mml:mi </mml:msub><mml:mo>·</mml:mo><ml:mn>2mathvariant="normal">H<mml:mn>2<td>1.1 ml:mn> < i</td><td>nml:msub></td></mml:mn></ml:mn></mml:mi </mml:mrow>	1.1 ml:mn> < i	nml:msub>
340	mathyariant="formal_shc/minimited sciences and the second science of the second science	1.5	21
341	Dual-Constrained Sulfur in FeS ₂ @C Nanostructured Lithium-Sulfide Batteries. ACS Applied Energy Materials, 2020, 3, 10950-10960.	2.5	21
342	Competition between tubular, planar and cage geometries: a complete picture of structural evolution of B _n (<i>n</i> = 31–50) clusters. Physical Chemistry Chemical Physics, 2020, 22, 12959-12966.	1.3	21

#	Article	IF	CITATIONS
343	2D tetragonal transition-metal phosphides: an ideal platform to screen metal shrouded crystals for multifunctional applications. Nanoscale, 2020, 12, 6776-6784.	2.8	21
344	Layer-dependent magnetic phase diagram in FenGeTe2 (3 ≤î ≤7) ultrathin films. Communications Physics, 2022, 5, .	2.0	21
345	Elastic and plastic deformations of nickel nanowires under uniaxial compression. Physica E: Low-Dimensional Systems and Nanostructures, 2005, 30, 45-50.	1.3	20
346	Stable Structures and Electronic Properties of the Oriented Bi Nanowires and Nanotubes from First-Principle Calculations. Journal of Physical Chemistry C, 2008, 112, 10745-10753.	1.5	20
347	Adsorption of selected gases on metal-organic frameworks and covalent organic frameworks: A comparative grand canonical Monte Carlo simulation. Journal of Applied Physics, 2012, 111, 112628.	1.1	20
348	Improved stability of water clusters (H2O)30–48: a Monte Carlo search coupled with DFT computations. Theoretical Chemistry Accounts, 2012, 131, 1.	0.5	20
349	Effects of Cr and W additions on the stability and migration of He in bcc Fe: A first-principles study. Computational Materials Science, 2016, 123, 85-92.	1.4	20
350	Structural evolution and magnetic properties of anionic clusters Cr ₂ Ge _{<i>n</i>} (<i>n</i> = 3–14): photoelectron spectroscopy and density functional theory compu Journal of Physics Condensed Matter, 2018, 30, 335501.	ut ati on.	20
351	Room temperature electrofreezing of water yields a missing dense ice phase in the phase diagram. Nature Communications, 2019, 10, 1925.	5.8	20
352	CO ₂ reduction on p-block metal oxide overlayers on metal substrates—2D MgO as a prototype. Journal of Materials Chemistry A, 2020, 8, 5688-5698.	5.2	20
353	Structural and electronic properties of germanium clathratesGe46andK8Ge46. Physical Review B, 1999, 60, 14177-14181.	1.1	19
354	Metallization of ZnO nanowires from partial hydrogen adsorption. Nanotechnology, 2007, 18, 455708.	1.3	19
355	Tuning bond contents in B–C–N films via temperature and bias voltage within RF magnetron sputtering. Surface and Coatings Technology, 2009, 204, 713-717.	2.2	19
356	Mechanical and electronic properties of ultrathin nanodiamonds under uniaxial compressions. Diamond and Related Materials, 2010, 19, 21-25.	1.8	19
357	Vacancy trapping mechanism for multiple hydrogen and helium in beryllium: a first-principles study. Journal of Physics Condensed Matter, 2012, 24, 095004.	0.7	19
358	Stability and Vibrations of Guest Molecules in the Type II Clathrate Hydrate: A First-Principles Study of Solid Phase. Journal of Physical Chemistry A, 2015, 119, 7063-7069.	1.1	19
359	Microstructure evolution and yield strength of CLAM steel in low irradiation condition. Materials Science & Engineering A: Structural Materials: Properties, Microstructure and Processing, 2017, 682, 563-568.	2.6	19
360	Atomistic understanding of the lateral growth of graphene from the edge of an h-BN domain: towards a sharp in-plane junction. Nanoscale, 2017, 9, 3585-3592.	2.8	19

#	Article	IF	CITATIONS
361	Tuning Schottky barriers for monolayer GaSe FETs by exploiting a weak Fermi level pinning effect. Physical Chemistry Chemical Physics, 2018, 20, 21732-21738.	1.3	19
362	First principles study of vacancy-solute complexes in vanadium. Journal of Alloys and Compounds, 2018, 763, 861-866.	2.8	19
363	Giant Thicknessâ€Tunable Bandgap and Robust Air Stability of 2D Palladium Diselenide. Small, 2020, 16, e2000754.	5.2	19
364	A nonorthogonal tight-binding total energy model for molecular simulations. Physics Letters, Section A: General, Atomic and Solid State Physics, 2003, 319, 523-529.	0.9	18
365	Structure Evolution of Transition Metal-doped Gold Clusters M@Au ₁₂ (M = 3d–5d): Across the Periodic Table. Journal of Physical Chemistry C, 2020, 124, 7449-7457.	1.5	18
366	Electronic and magnetic properties of ultrathin rhodium nanowires. Journal of Physics Condensed Matter, 2003, 15, 2327-2334.	0.7	17
367	Lowest-energy endohedral fullerene structure of Si60from a genetic algorithm and density-functional theory. Journal of Physics Condensed Matter, 2007, 19, 226208.	0.7	17
368	Novel Magnetic Monolayers of Transition Metal Silicide. Journal of Superconductivity and Novel Magnetism, 2015, 28, 1755-1758.	0.8	17
369	Electric field and strain tunable electronic structures in monolayer Black Phosphorus. Computational Materials Science, 2016, 112, 297-303.	1.4	17
370	Magnetism in the p-type Monolayer II-VI semiconductors SrS and SrSe. Scientific Reports, 2017, 7, 45869.	1.6	17
371	Dissociation mechanism of propane hydrate with methanol additive: A molecular dynamics simulation. Computational and Theoretical Chemistry, 2018, 1123, 79-86.	1.1	17
372	Revisit of largeâ€gap Si ₁₆ clusters encapsulating groupâ€ŀV metal atoms (Ti, Zr, Hf). Journal of Computational Chemistry, 2018, 39, 2268-2272.	1.5	17
373	Foreign atom encapsulated Au ₁₂ golden cages for catalysis of CO oxidation. Physical Chemistry Chemical Physics, 2019, 21, 10587-10593.	1.3	17
374	Robust spin manipulation in 2D organometallic Kagome lattices: a first-principles study. Physical Chemistry Chemical Physics, 2020, 22, 11045-11052.	1.3	17
375	Correlation between structures, ionization potentials and chemical reactivities of niobium clusters. Physics Letters, Section A: General, Atomic and Solid State Physics, 1996, 214, 211-214.	0.9	16
376	Surface thermal stability of nickel clusters. Physica Status Solidi (B): Basic Research, 1996, 193, 355-361.	0.7	16
377	Compressibility of liquid nitromethane in the high-pressure regime. Physica B: Condensed Matter, 2006, 382, 334-339.	1.3	16
378	Hydrogen storage behavior in C15 Laves phase compound TiCr2 by first principles. Journal of Applied Physics, 2009, 105, .	1.1	16

#	Article	IF	CITATIONS
379	A Topological method for global optimization of clusters: Application to (TiO ₂) <i>_n</i> (<i>n</i> = 1–6). Journal of Computational Chemistry, 2012, 33, 163-169.	1.5	16
380	An electrocatalyst with anti-oxidized capability for overall water splitting. Nano Research, 2018, 11, 3411-3418.	5.8	16
381	An ultralow-density porous ice with the largest internal cavity identified in the water phase diagram. Proceedings of the National Academy of Sciences of the United States of America, 2019, 116, 12684-12691.	3.3	16

Evolution of atomic structures of Sn<i>N</i>, Sn<i>N</i>â', and Sn<i>N</i>Clâ' clusters (<i>N</i> =) Tj ETQq0 0 Q rgBT /Overlock 10 T

382		1.2	16
383	Tunable bending modulus and bending limit of oxidized graphene. Nanoscale, 2020, 12, 1623-1628.	2.8	16
384	Atomic Wires of Transition Metal Chalcogenides: A Family of 1D Materials for Flexible Electronics and Spintronics. Jacs Au, 2021, 1, 147-155.	3.6	16
385	Temperature-dependent hardness of zinc-blende structured covalent materials. Science China Materials, 2021, 64, 2280-2288. Electronic properties and chemical trends of the arsenic <i>in situ</i> impurities in <mml:math< td=""><td>3.5</td><td>16</td></mml:math<>	3.5	16
386	xmlns:mml="http://www.w3.org/1998/Math/MathML" display="inline"> <mml:mrow><mml:msub><mml:mi mathvariant="normal">Hg<mml:mrow><mml:mn>1</mml:mn><mml:mo>â^`</mml:mo><mml:mi>xmathvariant="normal">Cd</mml:mi><mml:mi>x</mml:mi><forml:mi mathvariant="normal">Te</forml:mi </mml:mrow>: First-principles study. Physical Review</mml:mi </mml:msub></mml:mrow>	mml;mi>< 1.1	/mml:mrow: 15
387	B, 2007, 76, . First-principles study of atomic nitrogen solid with cubic gauche structure. Physics Letters, Section A: General, Atomic and Solid State Physics, 2007, 360, 645-648.	0.9	15
388	Stability and magnetic properties of Fe encapsulating in silicon nanotubes. Nanotechnology, 2007, 18, 235705.	1.3	15
389	Structure and mechanical properties of cubic BC2N crystals within a random solid solution model. Diamond and Related Materials, 2010, 19, 1419-1422.	1.8	15
390	Preparation of B–C–N films by magnetron sputtering with different N2/Ar flow ratio. Vacuum, 2011, 85, 887-891.	1.6	15
391	Adsorption of Aromatic Heterocyclic Compounds on Pristine and Defect Graphene: A First-Principles Study. Journal of Computational and Theoretical Nanoscience, 2011, 8, 2492-2497.	0.4	15
392	Synergetic effect of H and He with vacancy in vanadium solid from first-principles simulations. Nuclear Instruments & Methods in Physics Research B, 2013, 303, 75-80.	0.6	15
393	Insight into the initial oxidation of 4 <mml:math <br="" xmlns:mml="http://www.w3.org/1998/Math/MathML">display="inline"><mml:mi>H</mml:mi></mml:math> -SiC from first-principles thermodynamics. Physical Review B, 2013, 87, .	1.1	15
394	<i>Ab initio</i> calculations of mechanical properties of bcc W–Re–Os random alloys: effects of transmutation of W. Journal of Physics Condensed Matter, 2016, 28, 295501.	0.7	15
395	Phase diagrams for clathrate hydrates of methane, ethane, and propane from first-principles thermodynamics. Physical Chemistry Chemical Physics, 2016, 18, 3272-3279.	1.3	15
396	First-principles study of noble gas atoms in bcc Fe. Journal of Nuclear Materials, 2017, 492, 134-141.	1.3	15

#	Article	IF	CITATIONS
397	Structures and Spectroscopic Properties of F [–] (H ₂ O) _{<i>n</i>} with <i>n</i> = 1–10 Clusters from a Global Search Based On Density Functional Theory. Journal of Physical Chemistry A, 2018, 122, 3413-3422.	1.1	15
398	Three-dimensional phase field simulation of intragranular void formation and thermal conductivity in irradiated α-Fe. Journal of Materials Science, 2018, 53, 11002-11014.	1.7	15
399	Revisit the landscape of protonated water clusters H+(H2O)n with <i>n</i> = 10–17: An <i>ab initio</i> global search. Journal of Chemical Physics, 2018, 148, 174305.	1.2	15
400	Dithiol Self-Assembled Monolayer Based Electrochemical Surface Plasmon Resonance Optical Fiber Sensor for Selective Heavy Metal Ions Detection. Journal of Lightwave Technology, 2021, 39, 4034-4040.	2.7	15
401	<i>Ab initio</i> global optimization of clusters. Chemical Modelling, 2015, , 249-292.	0.2	15
402	Gas Adsorption of Carbon Nanotubes: Tube-Molecule Interaction and Technological Applications. Current Nanoscience, 2005, 1, 169-176.	0.7	15
403	Structure and ionization potential of coinage-metal clusters. Physics Letters, Section A: General, Atomic and Solid State Physics, 1994, 189, 223-226.	0.9	14
404	Mechanical behaviour of BC3compound and pure carbon nanotubes with topological defects. Nanotechnology, 2007, 18, 105705.	1.3	14
405	Study of high-pressure and high-temperature behaviors and α-to-β phase transition of forsterite by first-principles and quasi-harmonic Debye model. Computer Physics Communications, 2008, 179, 417-423.	3.0	14
406	Structural stability, mechanical and electronic properties of cubic BCxN crystals within a random solid solution model. Journal of Physics Condensed Matter, 2009, 21, 405401.	0.7	14
407	Solute/impurity diffusivities in bcc Fe: A first-principles study. Journal of Nuclear Materials, 2014, 455, 354-359.	1.3	14
408	Structural and electronic properties of the transition layer at the SiO2/4H-SiC interface. AIP Advances, 2015, 5, .	0.6	14
409	Atomic investigation of alloying Cr, Ti, Y additions in a grain boundary of vanadium. Journal of Nuclear Materials, 2016, 468, 147-152.	1.3	14
410	Enhanced thermoelectric properties of graphene oxide patterned by nanoroads. Physical Chemistry Chemical Physics, 2016, 18, 10607-10615.	1.3	14
411	Tailoring physical properties of graphene: Effects of hydrogenation, oxidation, and grain boundaries by atomistic simulations. Computational Materials Science, 2016, 112, 527-546.	1.4	14
412	Improved Finnis-Sinclair potential for vanadium-rich V–Ti–Cr ternary alloys. Journal of Alloys and Compounds, 2017, 705, 369-375.	2.8	14
413	Helium behavior in different oxides inside ODS steels: A comparative ab initio study. Journal of Nuclear Materials, 2018, 507, 101-111.	1.3	14
414	First-principles calculations of vacancy-O-He and vacancy-N-He complexes in vanadium. Computational Materials Science, 2019, 160, 180-185.	1.4	14

#	Article	IF	CITATIONS
415	Structures, stabilities and electronic properties of TimSiâ^'n (m = 1‒2, n = 14‒20) clusters: a combine initio and experimental study. European Physical Journal Plus, 2020, 135, 1.	ed ab 1.2	14
416	Imaging Vacancy Defects in Single-Layer Chromium Triiodide. Journal of Physical Chemistry Letters, 2021, 12, 2199-2205.	2.1	14
417	Tight-binding calculation of ionization potentials of small silicon clusters. Physics Letters, Section A: General, Atomic and Solid State Physics, 1995, 198, 243-247.	0.9	13
418	Density functional study of onion-skin-like [As@Ni12As20]3â^' and [Sb@Pd12Sb20]3â^' cluster ions. Chemical Physics Letters, 2004, 396, 161-166.	1.2	13
419	Thermal decomposition behaviour of RDX by first-principles molecular dynamics simulation. Molecular Simulation, 2008, 34, 961-965.	0.9	13
420	Most stable structures of polyhydroxylated endohedral metallofullerene Gd@C82(OH)x (x=1–24) from density function theory. Chemical Physics Letters, 2010, 492, 68-70.	1.2	13
421	Structural Evolution and Electronic Properties of Medium-Sized Gallium Clusters from <i>Ab Initio</i> Genetic Algorithm Search. Journal of Nanoscience and Nanotechnology, 2012, 12, 132-137.	0.9	13
422	Structural, electronic and elastic properties of several metal organic frameworks as a new kind of energetic materials. Chemical Physics Letters, 2015, 628, 76-80.	1.2	13
423	Bottom-up design of 2D organic photocatalysts for visible-light driven hydrogen evolution. Journal of Physics Condensed Matter, 2016, 28, 034004.	0.7	13
424	Multiscale Simulation of Yield Strength in Reduced-Activation Ferritic/Martensitic Steel. Nuclear Engineering and Technology, 2017, 49, 569-575.	1.1	13
425	Temperature and coverage effects on the stability of epitaxial silicene on Ag(111) surfaces. Applied Surface Science, 2017, 409, 97-101.	3.1	13
426	Medium-sized \${m Si}_{n}^{-}\$ (<i>n</i> =  14–20) clusters: a combined study of photoeled spectroscopy and DFT calculations. Journal of Physics Condensed Matter, 2018, 30, 354002.	tron 0.7	13
427	Dual transition metal doped germanium clusters for catalysis of CO oxidation. Journal of Alloys and Compounds, 2019, 806, 698-704.	2.8	13
428	Understanding the thermal conductivity of pristine W and W–Re alloys from a physics-based model. Journal of Nuclear Materials, 2020, 529, 151931.	1.3	13
429	Carrier Dynamics and Transfer across the CdS/MoS ₂ Interface upon Optical Excitation. Journal of Physical Chemistry Letters, 2020, 11, 6544-6550.	2.1	13
430	Control of Photocarrier Separation and Recombination at Bismuth Oxyhalide Interface for Nitrogen Fixation. Journal of Physical Chemistry Letters, 2020, 11, 9304-9312.	2.1	13
431	Effects of spin–phonon coupling on two-dimensional ferromagnetic semiconductors: a case study of iron and ruthenium trihalides. Nanoscale, 2021, 13, 7714-7722.	2.8	13
432	Size Dependence of the Ionization Potentials of Cd Clusters. Europhysics Letters, 1994, 28, 311-315.	0.7	12

#	Article	IF	CITATIONS
433	Raman scattering from LiF clusterâ€based nanophase film. Applied Physics Letters, 1995, 66, 523-525.	1.5	12
434	n-diamond from catalysed carbon nanotubes: synthesis and crystal structure. Journal of Physics Condensed Matter, 2005, 17, L513-L519.	0.7	12
435	Electronic properties of a silicon carbide nanotube under uniaxial tensile strain: a density function theory study. Journal of Nanoparticle Research, 2010, 12, 2919-2928.	0.8	12
436	Electromechanical properties of zigzag-shaped carbon nanotubes. Physical Chemistry Chemical Physics, 2013, 15, 17134.	1.3	12
437	Unreacted equation of states of typical energetic materials under static compression: A review. Chinese Physics B, 2016, 25, 076202.	0.7	12
438	A new family of multifunctional silicon clathrates: Optoelectronic and thermoelectric applications. Journal of Applied Physics, 2017, 121, .	1.1	12
439	Phase diagram of water–methane by first-principles thermodynamics: discovery of MH-IV and MH-V hydrates. Physical Chemistry Chemical Physics, 2017, 19, 15996-16002.	1.3	12
440	Design of superhalogens using a core–shell structure model. Nanoscale, 2017, 9, 18781-18787.	2.8	12
441	Stability of X-C-vacancy complexes (X=H, He) in vanadium from first principles investigations. Journal of Nuclear Materials, 2018, 505, 119-126.	1.3	12
442	Two-dimensional transition metal dichalcogenides as metal sources of metal–organic frameworks. Chemical Communications, 2018, 54, 3664-3667.	2.2	12
443	The pressure effects and vibrational properties of energetic material: Hexahydroâ€1,3,5â€ŧrinitroâ€1,3,5â€ŧriazine (<i>α</i> â€RDX). Journal of Raman Spectroscopy, 2019, 50, 889-8	9 1 .2	12
444	Determination of second- and third-order elastic constants for energetic materials. Computational Materials Science, 2019, 161, 379-384.	1.4	12
445	Atomistic understanding of helium behaviors at grain boundaries in vanadium. Computational Materials Science, 2019, 158, 296-306.	1.4	12
446	Metal-Encapsulated Boron Nitride Nanocages for Solar-Driven Nitrogen Fixation. Journal of Physical Chemistry C, 2020, 124, 23798-23806.	1.5	12
447	Experimental Realization of Two-Dimensional Buckled Lieb Lattice. Nano Letters, 2020, 20, 2537-2543.	4.5	12
448	Ferromagnetic Dirac half-metallicity in transition metal embedded honeycomb borophene. Physical Chemistry Chemical Physics, 2021, 23, 17150-17157.	1.3	12
449	Particle Swarm Predictions of a SrB ₈ Monolayer with 12-Fold Metal Coordination. Journal of the American Chemical Society, 2022, 144, 11120-11128.	6.6	12
450	MAGNETIC PROPERTIES OF ICOSAHEDRAL COPPER-COATED COBALT CLUSTERS. Surface Review and Letters, 2004, 11, 15-20.	0.5	11

#	Article	IF	CITATIONS
451	Electronic and magnetic properties of multishell Co nanowires coated with Cu. Solid State Communications, 2004, 129, 25-30.	0.9	11
452	Structural properties of silver nanowires from atomistic descriptions. Physical Review B, 2007, 76, .	1.1	11
453	Coupled effects of size and uniaxial force on phase transitions in copper nanowires. Nanotechnology, 2010, 21, 185703.	1.3	11
454	Numerical simulation of the combined effects of plasma heating and neutron heating loads on the ITER first wall. Fusion Engineering and Design, 2011, 86, 45-50.	1.0	11
455	First-principles calculations of elastic moduli of Ti–Mo–Nb alloys using a cluster-plus-glue-atom model for stable solid solutions. Journal of Materials Science, 2013, 48, 3138-3146.	1.7	11
456	Observation of He bubbles in ion irradiated fusion materials by conductive atomic force microscopy. Journal of Nuclear Materials, 2013, 441, 54-58.	1.3	11
457	Evolution of boron clusters in iron tetraborides under high pressure: semiconducting and ferromagnetic superhard materials. RSC Advances, 2015, 5, 48012-48023.	1.7	11
458	A Gupta potential for magnesium in hcp phase. Computational Materials Science, 2015, 98, 328-332.	1.4	11
459	A strain or electric field induced direct bandgap in ultrathin silicon film and its application in photovoltaics or photocatalysis. Physical Chemistry Chemical Physics, 2016, 18, 7156-7162.	1.3	11
460	Diffusion and retention of hydrogen in vanadium in presence of Ti and Cr: First-principles investigations. Journal of Nuclear Materials, 2017, 484, 276-282.	1.3	11
461	Understanding the mechanical properties of reduced activation steels. Materials and Design, 2018, 146, 260-272.	3.3	11
462	Large magnetic anisotropy in chemically engineered iridium dimer. Communications Physics, 2018, 1, .	2.0	11
463	Monolayered semiconducting GeAsSe and SnSbTe with ultrahigh hole mobility. Frontiers of Physics, 2018, 13, 1.	2.4	11
464	First principles investigations of hydrogen interaction with vacancy-oxygen complexes in vanadium alloys. International Journal of Hydrogen Energy, 2019, 44, 26637-26645.	3.8	11
465	Remarkable Role of Grain Boundaries in the Thermal Transport Properties of Phosphorene. ACS Omega, 2020, 5, 17416-17422.	1.6	11
466	Oxidation Behaviors of Twoâ€dimensional Metal Chalcogenides. ChemNanoMat, 2020, 6, 838-849.	1.5	11
467	Enhanced Valley Polarization of Bilayer MoSe ₂ with Variable Stacking Order and Interlayer Coupling. Journal of Physical Chemistry Letters, 2021, 12, 5879-5888.	2.1	11
468	A B ₂ N monolayer: a direct band gap semiconductor with high and highly anisotropic carrier mobility. Nanoscale, 2022, 14, 930-938.	2.8	11

#	Article	IF	CITATIONS
469	Photoinduced Spin Injection and Ferromagnetism in 2D Group III Monochalcogenides. Journal of Physical Chemistry Letters, 2022, 13, 590-597.	2.1	11
470	An analytic relationship between size and ionization potential of transition-metal clusters. Chemical Physics Letters, 1996, 254, 21-24.	1.2	10
471	Structural, electronic, and optical properties of medium-sized Lin clusters (n=20, 30, 40, 50) by density functional theory. Physica E: Low-Dimensional Systems and Nanostructures, 2010, 42, 1755-1762.	1.3	10
472	A first-principle study of the structural and electronic properties of amorphous Cu-Zr alloys. Science China: Physics, Mechanics and Astronomy, 2011, 54, 249-255.	2.0	10
473	Tunable deformation and electronic properties of single-walled ZnO nanotubes under a transverse electric field. Journal of Applied Physics, 2012, 111, 073704.	1.1	10
474	Gupta potential for rare earth elements of the fcc phase: lanthanum and cerium. Modelling and Simulation in Materials Science and Engineering, 2013, 21, 065003.	0.8	10
475	Structures and electronic properties of neutral and anionic Ca (n= 2–22) clusters. Chemical Physics Letters, 2015, 634, 255-260.	1.2	10
476	Structures, Stabilities, and Spectra Properties of Fused CH ₄ Endohedral Water Cage (CH ₄) _{<i>m</i>} (H ₂ O) _{<i>n</i>} Clusters from DFT-D Methods. Journal of Physical Chemistry A, 2015, 119, 10971-10979.	1.1	10
477	Effect of interstitial impurities on grain boundary cohesive strength in vanadium. Computational Materials Science, 2015, 110, 163-168.	1.4	10
478	Magnetism and energetics for vacancy and helium impurity in Fe-9Cr alloy: A first-principles study. Computational Materials Science, 2017, 138, 267-276.	1.4	10
479	Effect of Ti/Cr additive on helium diffusion and segregation in dilute vanadium alloys. Nuclear Instruments & Methods in Physics Research B, 2017, 393, 130-134.	0.6	10
480	Interactions between helium, hydrogen and intrinsic point defects in TaC crystal. Journal of Alloys and Compounds, 2018, 741, 900-907.	2.8	10
481	Three dimensional porous SiC for lithium polysulfide trapping. Physical Chemistry Chemical Physics, 2018, 20, 4005-4011.	1.3	10
482	Helium behavior in oxide dispersion strengthened (ODS) steel: Insights from ab initio modeling. Journal of Nuclear Materials, 2018, 499, 71-78.	1.3	10
483	Rational design of 2D organic magnets with giant magnetic anisotropy based on two-coordinate 5d transition metals. APL Materials, 2020, 8, .	2.2	10
484	Electric-Field-Driven Negative Differential Conductance in 2D van der Waals Ferromagnet Fe ₃ GeTe ₂ . Nano Letters, 2021, 21, 9233-9239.	4.5	10
485	Transition metal halide nanowires: A family of one-dimensional multifunctional building blocks. Applied Physics Letters, 2022, 120, .	1.5	10
486	Enhanced Fluorescence with Tunable Color in Doped Diphosphine-Protected Gold Nanoclusters. Journal of Physical Chemistry Letters, 2022, 13, 5873-5880.	2.1	10

#	Article	IF	CITATIONS
487	Instabilities in cubic diamond under non-hydrostatic compressive stress. Diamond and Related Materials, 2008, 17, 1353-1355.	1.8	9
488	Hydrogen storage behavior of one-dimensional TiB _{<i>x</i>} chains. Nanotechnology, 2010, 21, 134006.	1.3	9
489	A theoretical evaluation of the effect of interlayer spacing and boron doping on lithium storage in graphite. Computational Materials Science, 2013, 68, 212-217.	1.4	9
490	Energetics and configurations of He–He pair in vacancy of transition metals. Nuclear Instruments & Methods in Physics Research B, 2014, 322, 34-40.	0.6	9
491	Anomalous ideal tensile strength of ferromagnetic Fe and Fe-rich alloys. Physical Review B, 2014, 90, .	1.1	9
492	Tensile strain-induced softening of iron at high temperature. Scientific Reports, 2015, 5, 16654.	1.6	9
493	Alloying effect on the ideal tensile strength of ferromagnetic and paramagnetic bcc iron. Journal of Alloys and Compounds, 2016, 676, 565-574.	2.8	9
494	Mechanical anisotropy and strain-tailored band structures of pentagonal boron nitride monolayers. Journal of Applied Physics, 2017, 122, 094302.	1.1	9
495	Strongly Hole-Doped and Highly Decoupled Graphene on Platinum by Water Intercalation. Journal of Physical Chemistry Letters, 2019, 10, 3998-4002.	2.1	9
496	Atomic Structures and Electronic Properties of Large-Sized GeN Clusters (N = 45, 50, 55, 60, 65, 70) by First-Principles Global Search. Journal of Cluster Science, 2019, 30, 371-377.	1.7	9
497	Three-dimensional borophene: A light-element topological nodal-line semimetal with direction-dependent type-II Weyl fermions. Physical Review B, 2020, 102, .	1.1	9
498	New refractory MAB phases and their 2D derivatives: insight into the effects of valence electron concentration and chemical composition. RSC Advances, 2020, 10, 25836-25847.	1.7	9
499	First-principles study of the Σ3(112) grain boundary in Fe-rich Fe-Cr alloys. Scripta Materialia, 2020, 181, 140-143.	2.6	9
500	Aminomethylâ€Functionalized Carbon Nanotubes as a Host of Small Sulfur Clusters for Highâ€Performance Lithium–Sulfur Batteries. ChemSusChem, 2020, 13, 2761-2768.	3.6	9
501	Numerical simulations of thermal conductivity in void-containing tungsten: Topological feature of voids. Journal of Nuclear Materials, 2021, 543, 152601.	1.3	9
502	Intrinsic spin–valley-coupled Dirac state in Janus functionalized β-BiAs monolayer. Nanoscale Horizons, 2021, 6, 283-289.	4.1	9
503	Single O Atom Doped Ag Cluster Cations for CO Oxidation: An O-Doped Superatom Ag ₁₅ O ⁺ with Remarkable Stability. Journal of Physical Chemistry C, 2021, 125, 7067-7076.	1.5	9
504	Interactions of solute atoms with self-interstitial atoms/clusters in vanadium: A first-principles study. Journal of Nuclear Materials, 2021, 553, 153055.	1.3	9

#	Article	IF	CITATIONS
505	Ultraviolet Optical Absorption Spectra of Water Clusters: From Molecular Dimer to Nanoscaled Cage-Like Hexakaidecahedron. Journal of Computational and Theoretical Nanoscience, 2007, 4, 453-466.	0.4	9
506	Eliminating Edge Electronic and Phonon States of Phosphorene Nanoribbon by Unique Edge Reconstruction. Small, 2022, 18, e2105130.	5.2	9
507	Prediction of superconductivity in bilayer borophenes. RSC Advances, 2021, 11, 40220-40227.	1.7	9
508	Transition-Metal Interlink Neural Network: Machine Learning of 2D Metal–Organic Frameworks with High Magnetic Anisotropy. ACS Applied Materials & Interfaces, 2022, 14, 33726-33733.	4.0	9
509	Chemisorption of Co monolayer on H-passivated Si(111) surface: Comparison with clean Si(111) surface. Chemical Physics Letters, 2005, 414, 500-504.	1.2	8
510	Insertion of C ₅₀ into singleâ€walled carbon nanotubes: Selectivity in interwall spacing and C ₅₀ isomers. Journal of Computational Chemistry, 2008, 29, 781-787.	1.5	8
511	Lowest-energy structures and photoelectron spectra of InnPn (n=1–12) clusters from density functional theory. Computational and Theoretical Chemistry, 2008, 862, 133-137.	1.5	8
512	Numerical simulation of the temperature field in laser-driven flyer plates by high power nanosecond laser–material interactions. Journal Physics D: Applied Physics, 2009, 42, 225302.	1.3	8
513	Theoretical identification of the lowest-energy structure of (SiC)12 heterocluster: Segregation of C and Si in planar and cage structures. Chemical Physics, 2009, 355, 31-36.	0.9	8
514	Infrared spectra of hydrogenated nanodiamonds by first-principles simulations. Physica E: Low-Dimensional Systems and Nanostructures, 2009, 41, 1427-1432.	1.3	8
515	Elastic behavior of (MgxFe1â^'x)2SiO4 olivine at high pressure from first-principles simulations. Journal of Physics and Chemistry of Solids, 2010, 71, 1094-1097.	1.9	8
516	The maximum number of carbonyl groups around an Ru6C polyhedral cluster: hexanuclear ruthenium carbonyl carbides. Dalton Transactions, 2010, 39, 10697.	1.6	8
517	First-principles study of the binary Ni60Ta40 metallic glass: The atomic structure and elastic properties. Journal of Non-Crystalline Solids, 2012, 358, 1730-1734.	1.5	8
518	Improved Finnis–Sinclair potential for bcc vanadium solid. Computational Materials Science, 2012, 53, 101-104.	1.4	8
519	Effect of helium and vacancies in a vanadium grain boundary by first-principles. Nuclear Instruments & Methods in Physics Research B, 2015, 352, 121-124.	0.6	8
520	Mesoscale modeling of irradiation damage evolution in bcc iron and vanadium: A comparative study. Fusion Engineering and Design, 2018, 137, 303-311.	1.0	8
521	Tuning the structures of two-dimensional cuprous oxide confined on Au(111). Nano Research, 2018, 11, 5957-5967.	5.8	8
522	Compositionally Designed 2D Ruddlesden–Popper Perovskites for Efficient and Stable Solar Cells. Solar Rrl, 2021, 5, 2000661.	3.1	8

#	Article	IF	CITATIONS
523	Selective CO2 conversion tuned by periodicities in Au8n+4(TBBT)4n+8 nanoclusters. Nano Research, 2021, 14, 807-813.	5.8	8
524	New boron nitride monolith phases from high-pressure compression of double-walled boron nitride nanotubes. Journal of Chemical Physics, 2021, 154, 134702.	1.2	8
525	Ab initio analytic calculation of point defects in AlGaN/GaN heterointerfaces. Journal of Physics Condensed Matter, 2021, 33, 035002.	0.7	8
526	Electrical Conductance of Graphene with Point Defects. Wuli Huaxue Xuebao/ Acta Physico - Chimica Sinica, 2019, 35, 1142-1149.	2.2	8
527	FeSi ₂ : a two-dimensional ferromagnet containing planar hexacoordinate Fe atoms. Nanoscale Advances, 2022, 4, 600-607.	2.2	8
528	Dramatically Enhanced Second Harmonic Generation in Janus Groupâ€III Chalcogenide Monolayers. Advanced Optical Materials, 2022, 10, .	3.6	8
529	Blue shift of plasma resonance of copper nanoclusters embedded in LiF. Journal of Physics and Chemistry of Solids, 1996, 57, 225-227.	1.9	7
530	Elastic Properties of Molecular Crystals Using Density Functional Calculations. AIP Conference Proceedings, 2004, , .	0.3	7
531	Optical properties of amorphous Ill–V compound semiconductors from first principles study. Solid State Communications, 2009, 149, 638-640.	0.9	7
532	Structural evolution of Aun (n=29–35) clusters: A transition from hollow cage to amorphous packing. Computational Materials Science, 2011, 50, 2359-2362.	1.4	7
533	Quantum conductance of armchair carbon nanocoils: roles of geometry effects. Science China: Physics, Mechanics and Astronomy, 2011, 54, 841-845.	2.0	7
534	Effect of iron on high pressure elasticity of hydrous wadsleyite and ringwoodite by first-principles simulation. High Pressure Research, 2012, 32, 385-395.	0.4	7
535	Ground state structures, electronic and optical properties of medium-sized Nan + (n = 9, 15, 21, 26, 31,) Tj ETQq1	10.7843 0.6	814 rgBT /O
536	Oxidation of step edges on vicinal 4H-SiC(0001) surfaces. Applied Physics Letters, 2013, 103, 211603.	1.5	7
537	Dissociation mechanism of gas hydrates (I, II, H) of alkane molecules: a comparative molecular dynamics simulation. Molecular Simulation, 2015, 41, 1086-1094.	0.9	7
538	Magnetic Anisotropy of Small Irn Clusters (nÂ=Â2–5). Journal of Cluster Science, 2016, 27, 935-946.	1.7	7
539	Plasma facing component with built-in tungsten wires and a W-Cu functionally graded layer: A finite element assessment. Fusion Engineering and Design, 2017, 120, 9-14.	1.0	7
540	Uniaxial compression behavior and spectroscopic properties of energetic 1,1-diamino-2,2-dinitroethylene (FOX-7) crystals from density functional theory calculations. Progress in Natural Science: Materials International, 2019, 29, 329-334.	1.8	7

#	Article	IF	CITATIONS
541	Two-dimensional cyclohexane methylamine based perovskites as stable light absorbers for solar cells. Solar Energy, 2020, 201, 13-20.	2.9	7
542	A mechanism-based quantitative multi-scale framework for investigating irradiation hardening of tungsten at low temperature. Materials Science & Engineering A: Structural Materials: Properties, Microstructure and Processing, 2020, 774, 138941.	2.6	7
543	The influence of temperature on the elastic properties of body-centered cubic reduced activation steels. Materials and Design, 2021, 197, 109282.	3.3	7
544	Searching for cluster Lego blocks for three-dimensional and two-dimensional assemblies. Physical Review Materials, 2021, 5, .	0.9	7
545	The reactivity of O2 with copper cluster anions Cuâ^' (nÂ=Â7â^'20): Leveling effect of spin accommodation. Chinese Chemical Letters, 2022, 33, 995-1000.	4.8	7
546	Topologically protected states and half-metal behaviors: Defect-strain synergy effects in two-dimensional antimonene. Physical Review Materials, 2019, 3, .	0.9	7
547	Compositionâ€Dependent Magnetic Ordering in Freestanding 2D Nonâ€van der Waals Cr ₂ Te <i>_x</i> Se _{3â^`} <i>_x</i> Crystals. Advanced Functional Materials, 2022, 32, .	7.8	7
548	FIRST-PRINCIPLES STUDY OF STRUCTURES AND ELECTRONIC PROPERTIES FOR NITRIDE-DOPED ALUMINUM CLUSTERS. International Journal of Modern Physics B, 2005, 19, 2380-2385.	1.0	6
549	Shell structures of sodium nanowires from atomistic simulations. Physical Review B, 2006, 74, .	1.1	6
550	Density Functional Theory Calculations of Water Fullerenes: (H ₂ O) _{<i>n</i>} Clusters with <i>n</i> = 20–40. Journal of Computational and Theoretical Nanoscience, 2009, 6, 454-458.	0.4	6
551	Mapping distributions of mechanical properties and formation ability on the ternary B―C―N phase diagram. Diamond and Related Materials, 2011, 20, 891-895.	1.8	6
552	Competition Between Core–Shell and Hollow Cage Structures in the Ga _{<i>n</i>} As _{<i>n</i>} (<i>n</i> = 10–15) Clusters. Journal of Computational and Theoretical Nanoscience, 2011, 8, 2488-2491.	0.4	6
553	Structural and mechanical properties of low-density amorphous carbon nitrides by molecular dynamics simulations. Diamond and Related Materials, 2012, 23, 44-49.	1.8	6
554	Tuning the electronic and optical properties of hydrogen-terminated Si nanocluster by uniaxial compression. Journal of Nanoparticle Research, 2012, 14, 1.	0.8	6
555	Relationship between chemical compositions of magnetron sputtered B–C–N films and various experimental parameters. Vacuum, 2012, 86, 1499-1504.	1.6	6
556	Carbon clusters near the step of Rh surface: implication for the initial stage of graphene nucleation. European Physical Journal D, 2013, 67, 1.	0.6	6
557	Ab initio calculations of elastic properties of Fe–Cr–W alloys. Computational Materials Science, 2014, 84, 301-305.	1.4	6
558	Solvent-Based Atomistic Theory for Doping Colloidal-Synthesized Quantum Dots via Cation Exchange. Journal of Physical Chemistry C, 2016, 120, 27085-27090.	1.5	6

#	Article	IF	CITATIONS
559	Gupta potentials for five HCP rare earth metals. Computational Materials Science, 2016, 112, 75-79.	1.4	6
560	Low-Energy Structures and Electronic Properties of Large-Sized Si _{<i>N</i>} Clusters (<i>N</i> = 60, 80, 100, 120, 150, 170). Journal of Physical Chemistry C, 2018, 122, 11086-11095.	1.5	6
561	Interaction Mechanisms of Insensitive Explosive FOX-7 and Graphene Oxides from Ab Initio Calculations. Nanomaterials, 2019, 9, 1290.	1.9	6
562	Electronic structures and charge carrier mobilities of boron-graphdiyne sheet and nanoribbons. Physica E: Low-Dimensional Systems and Nanostructures, 2020, 124, 114354.	1.3	6
563	Solar driven CO2 hydrogenation on transition metal doped Zn12O12 cluster. Journal of Chemical Physics, 2020, 153, 164306.	1.2	6
564	Ground-State Structures of Hydrated Calcium Ion Clusters From Comprehensive Genetic Algorithm Search. Frontiers in Chemistry, 2021, 9, 637750.	1.8	6
565	Magnetic field modulated photoelectric devices in ferromagnetic semiconductor CrXh (X =) Tj ETQq1 1	0.784314 1.5	rgBT /Overic
566	Investigation of electronic and vibrational properties of dihydroxylammonium 5,5′-bistetrazole-1,1′-diolate under high-pressure conditions. Physical Chemistry Chemical Physics, 2021, 23, 7442-7448.	1.3	6
567	Intrinsic Multiferroic in VNI Monolayer. ACS Applied Electronic Materials, 2022, 4, 3177-3182.	2.0	6
568	Conductance resonance of metalâ€insulatorâ€metal junction with embedded metal cluster. Applied Physics Letters, 1994, 65, 2419-2421.	1.5	5
569	Magic numbers and a growth pathway of high-nuclearity titanium carbide clusters. Solid State Communications, 2002, 124, 253-256.	0.9	5
570	Calculations of electronic structure ofGe44Mn2Ba8andGe42Mn4Ba8clathrates. Physical Review B, 2004, 70, .	1.1	5
571	Hexanuclear Cobalt Carbonyl Carbide Clusters: The Interplay between Octahedral and Trigonal Prismatic Structures. Inorganic Chemistry, 2008, 47, 9314-9320.	1.9	5
572	Nonclassical Cn (n=30–40, 50) fullerenes containing five-, six-, seven-member rings. Computational and Theoretical Chemistry, 2011, 969, 35-43.	1.1	5
573	Toroidal and Coiled Carbon Nanotubes. , 0, , .		5
574	Graphene antidot lattices as potential electrode materials for supercapacitors. Physica E: Low-Dimensional Systems and Nanostructures, 2015, 69, 316-321.	1.3	5
575	Revisit of Sin (nÂ=Â21–29) Clusters by Ab Initio Global Search. Journal of Cluster Science, 2017, 28, 1729-1737.	1.7	5
576	Quantum oscillation in carrier transport in two-dimensional junctions. Nanoscale, 2018, 10, 7912-7917.	2.8	5

#	Article	IF	CITATIONS
577	Electronic and magnetic properties of transition metal decorated monolayer GaS. Physica E: Low-Dimensional Systems and Nanostructures, 2018, 101, 131-138.	1.3	5
578	Phase Diagram of Methane Hydrates and Discovery of MH-VI Hydrate. Journal of Physical Chemistry A, 2018, 122, 6007-6013.	1.1	5
579	The effect of Cr on He segregation and diffusion at Σ3(1 1 2) grain boundary in α-Fe. Nuclear Instruments & Methods in Physics Research B, 2019, 456, 7-11.	0.6	5
580	First-principles investigation of hydrogen behavior in different oxides in ODS steels. International Journal of Hydrogen Energy, 2019, 44, 17105-17113.	3.8	5
581	Materials selection for nuclear applications in view of divacancy energies by comprehensive first-principles calculations. Journal of Nuclear Materials, 2020, 538, 152253.	1.3	5
582	First-Principles Calculations for Stable β-Ti–Mo Alloys Using Cluster-Plus-Glue-Atom Model. Acta Metallurgica Sinica (English Letters), 2020, 33, 968-974.	1.5	5
583	A first-principles study of helium diffusion in quartz and coesite under high pressure up to 12GPa. Geoscience Frontiers, 2021, 12, 1001-1009.	4.3	5
584	Multiscale simulations of the hydration shells surrounding spherical Fe ₃ O ₄ nanoparticles and effect on magnetic properties. Nanoscale, 2021, 13, 9293-9302.	2.8	5
585	Transition metal-doped Bn (n = 7â^'10) clusters: confirmation of a circular disk Jellium model. European Physical Journal Plus, 2021, 136, 1.	1.2	5
586	Universal Zigzag Edge Reconstruction of an α-Phase Puckered Monolayer and Its Resulting Robust Spatial Charge Separation. Nano Letters, 2021, 21, 8095-8102.	4.5	5
587	Methane conversion by transition metal-doped vanadium oxide clusters. Chemical Physics Letters, 2021, 779, 138829.	1.2	5
588	Evolution of Water Layer Adsorption on the GaN(0001) Surface and Its Influence on Electronic Properties. Journal of Physical Chemistry C, 2021, 125, 667-674.	1.5	5
589	Stability and NMR Chemical Shift of Amorphous Precursors of Methane Hydrate: Insights from Dispersion-Corrected Density Functional Theory Calculations Combined with Machine Learning. Journal of Physical Chemistry B, 2021, 125, 431-441.	1.2	5
590	Robust Dirac spin gapless semiconductors in a two-dimensional oxalate based organic honeycomb-kagome lattice. Nanoscale, 2022, 14, 2023-2029.	2.8	5
591	Modeling irradiation-induced intragranular gas bubble in tungsten under external tensile loading. International Journal of Refractory Metals and Hard Materials, 2022, 105, 105824. Two-dimensional oxides assembled by <mml:math< td=""><td>1.7</td><td>5</td></mml:math<>	1.7	5
592	xmlns:mml="http://www.w3.org/1998/Math/MathML"> <mml:msub><mml:mi>M</mml:mi><mml:mn>4</mml:mn> clusters (<mml:math) (xmlns:mml="http://www.w3.org/1998/Math/N</td><td>> </mml:m
MathML" 0="" 10="" 142="" 50="" :<br="" etqq0="" overlock="" rgbt="" td="" tf="" tj="">1.3</mml:math)></mml:msub>	sub>, <mml:mrov< td=""></mml:mrov<>	
593	Review Research, 2021, 3, .		

#	Article	IF	CITATIONS
595	A modified Hückel calculation on the structures and ionization potentials of Ag clusters. Physica Status Solidi (B): Basic Research, 1995, 188, 719-722.	0.7	4
596	Time-evolutional X-ray diffraction of n-diamond: An intermediate state between fcc and diamond structure. Diamond and Related Materials, 2006, 15, 1323-1328.	1.8	4
597	First-principles study of the effect of water on the phase transitions in Mg ₂ SiO ₄ forsterite. High Pressure Research, 2010, 30, 318-324.	0.4	4
598	Stability and mechanical properties of BC _{<i>x</i>} crystals: the role of B–B bonds and boron concentration. Journal of Physics Condensed Matter, 2010, 22, 215401.	0.7	4
599	Gupta potential for alkaline earth metals: Calcium and strontium. Computational Materials Science, 2014, 85, 142-146.	1.4	4
600	Elastic anharmonicity of bcc Fe and Fe-based random alloys from first-principles calculations. Physical Review B, 2017, 95, .	1.1	4
601	Prediction of huge magnetic anisotropies in 5 <i>d</i> transition metallocenes. Journal of Physics Condensed Matter, 2017, 29, 435802.	0.7	4
602	Compression behavior and spectroscopic properties of insensitive explosive 1,3,5-triamino-2,4,6-trinitrobenzene from dispersion-corrected density functional theory. Chinese Physics B, 2018, 27, 056401.	0.7	4
603	Uniaxial compression behavior and spectroscopic properties of the explosive pentaerythritol tetranitrate from first-principles calculations. Computational Materials Science, 2018, 153, 392-398.	1.4	4
604	Compressive behavior and electronic properties of ammonia ice: a first-principles study. RSC Advances, 2020, 10, 26579-26587.	1.7	4
605	Matching vacancy formation energy and defect levels with the density of amorphous Ga2O3. Journal of Materials Science, 2020, 55, 9343-9353.	1.7	4
606	Structures and vertical detachment energies of water cluster anions (H2O)â^'n with n = 6–11. Theoretical Chemistry Accounts, 2020, 139, 1.	0.5	4
607	Novel Carbon Nanotube Peapods Encapsulating Au ₃₂ Golden Fullerene. Journal of Computational and Theoretical Nanoscience, 2006, 3, 459-462.	0.4	4
608	Nonlinear Properties of Nanometer-Sized Copper Clusters Embedded in LiF Medium. Japanese Journal of Applied Physics, 1995, 34, 53.	0.8	4
609	First-principles calculations of transition elements interaction with hydrogen in vanadium. Journal of Nuclear Materials, 2022, 564, 153710.	1.3	4
610	Phonon-Assisted Nonradiative Recombination Tuned by Organic Cations in Ruddlesden-Popper Hybrid Perovskites. Physical Review Applied, 2022, 17, .	1.5	4
611	Multiple-channel resonant tunneling in a tunneling junction with an impurity cluster. Physical Review B, 1996, 53, 7842-7846.	1.1	3
612	First-Principles Studies of RDX Crystals under Compression. AlP Conference Proceedings, 2006, , .	0.3	3

#	Article	IF	CITATIONS
613	Interactions of extrinsic interstitial atoms (H, He, O, C) with vacancies in beryllium from first-principles. Computational Materials Science, 2014, 90, 116-122.	1.4	3
614	Effect of Hydrogen in a Vanadium Grain Boundary by First Principles. Fusion Science and Technology, 2014, 66, 106-111.	0.6	3
615	Application of GO in Environmental Science. SpringerBriefs in Physics, 2015, , 119-135.	0.2	3
616	Thermal–Mechanical Responses of the First Wall in CFETR Under Transient Events. Journal of Fusion Energy, 2017, 36, 49-57.	0.5	3
617	Viscoplastic equations incorporated into a finite element model to predict deformation behavior of irradiated reduced activation ferritic/martensitic steel. Fusion Engineering and Design, 2017, 118, 129-134.	1.0	3
618	Self-assembly 2D zinc-phthalocyanine heterojunction: An ideal platform for high efficiency solar cell. Applied Physics Letters, 2017, 111, 253904.	1.5	3
619	Two dimensional self-assembly zinc porphyrin and zinc phthalocyanine heterojunctions with record high power conversion efficiencies. Journal of Physics Condensed Matter, 2018, 30, 25LT02.	0.7	3
620	First-principles investigations of intrinsic point defects and helium impurities in vanadium monocarbide. Nuclear Instruments & Methods in Physics Research B, 2020, 479, 163-170.	0.6	3
621	Oxygen interaction with alloying elements (Cr/Ni) and vacancies in dilute austenitic iron alloys: A first-principles study. Fusion Engineering and Design, 2021, 163, 112123.	1.0	3
622	First-principles explorations on P ₈ and N ₂ assembled nanowire and nanowire and nanosheet. Nano Express, 2021, 2, 010004.	1.2	3
623	Thermal properties of energetic materials from quasi-harmonic first-principles calculations. Journal of Physics Condensed Matter, 2021, 33, 275702.	0.7	3
624	Effects of Cr and Ti additions on the stability and migration of C, N and O in vanadium: A first-principles study. Fusion Engineering and Design, 2021, 168, 112604.	1.0	3
625	Bimetal single-molecule magnets supported on benzene with large magnetic anisotropy and unquenched orbital moment. Physical Review Research, 2021, 3, .	1.3	3
626	Examining deformation localization of irradiated tungsten under uniaxial compression with crystal plasticity. International Journal of Refractory Metals and Hard Materials, 2021, 100, 105637.	1.7	3
627	Superior flexibility of planar graphene allotropes with pentagons and heptagons. Applied Surface Science, 2021, 569, 151048.	3.1	3
628	Structural Modeling and Physical Properties. SpringerBriefs in Physics, 2015, , 31-56.	0.2	3
629	Tuning Optical Absorption and Emission of Sub-Nanometer Gold-Caged Metal Systems M@Au ₁₄ by Substitutional Doping. Journal of Computational and Theoretical Nanoscience, 2006, 3, 312-314.	0.4	3
630	Compression Behavior and Vibrational Properties of New Energetic Material LLM-105 Analyzed Using the Dispersion-Corrected Density Functional Theory. Molecules, 2021, 26, 6831.	1.7	3

#	Article	IF	CITATIONS
631	Phase Diagrams and Spectral Characteristics of Hydrofluorocarbon Hydrates: Insights from First-Principles Thermodynamics. ACS Sustainable Chemistry and Engineering, 2021, 9, 16347-16355.	3.2	3
632	Theoretical insights of structural evolution and electronic properties of Ru2Gen (n = 1–16) clusters. European Physical Journal Plus, 2022, 137, 1.	1.2	3
633	Inverse Design of Nanoclusters for Light-Controlled CO ₂ –HCOOH Interconversion. Journal of Physical Chemistry Letters, 2022, 13, 2523-2532.	2.1	3
634	Electronic properties in the interaction random-cluster model. Physics Letters, Section A: General, Atomic and Solid State Physics, 1995, 204, 169-173.	0.9	2
635	Structure of Medium-Sized Au Clusters by First-Principles. Journal of Computational and Theoretical Nanoscience, 2009, 6, 318-326.	0.4	2
636	Optical property of amorphous semiconductor mercury cadmium telluride from first-principles study. Science in China Series D: Earth Sciences, 2009, 52, 1928-1932.	0.9	2
637	Searching superhard cubic phases in ternary B–C–N phase diagram using first-principles calculations. Diamond and Related Materials, 2012, 27-28, 14-18.	1.8	2
638	Lowest-energy cage structures of medium-sized (ZnO)n clusters with n = 15 â^ 24. , 2015, , .		2
639	Pressure dependence on electronic structures, charge distribution and bond orders of solid nitromethane using nonlocal DFT functional. Molecular Simulation, 2018, 44, 1454-1460.	0.9	2
640	Helium behaviors at Mn6Ni16Si7 precipitate in α-Fe: Insights from ab initio modeling. Computational Materials Science, 2020, 181, 109735.	1.4	2
641	Ab initio study of He, Ne, Ar, Kr incorporation in zirconium carbide. Journal of Nuclear Materials, 2020, 534, 152154.	1.3	2
642	Ab initio modelling of helium behavior in α-Fe/TaC interface. Nuclear Materials and Energy, 2021, 27, 100956.	0.6	2
643	Compression behavior of energetic ε â€CLâ€20 crystals from density functional theory calculations. Journal of Raman Spectroscopy, 2021, 52, 1764.	1.2	2
644	A valence balancing rule for the design of bimetallic phosphides targeting high thermoelectric performance. Physical Chemistry Chemical Physics, 2021, 23, 18916-18924.	1.3	2
645	Fabrication and Reduction. SpringerBriefs in Physics, 2015, , 1-13.	0.2	2
646	Tight-binding Calculation of Size Dependence of the Ionisation Potentials of Mercury Clusters. Australian Journal of Physics, 1995, 48, 731.	0.6	2
647	Heat transfer analysis of irradiation-induced gas bubble in tungsten from a fractal dimension perspective. International Journal of Heat and Mass Transfer, 2022, 193, 122965.	2.5	2
648	Effects of vacancy defects on the magnetic properties of vanadium diselenide monolayers: a first principle investigation. Physical Chemistry Chemical Physics, 2022, 24, 17615-17622.	1.3	2

#	Article	IF	CITATIONS
649	STRUCTURAL AND RAMAN SPECTRA STUDIES OF SUPPORTED LIF CLUSTERS. Surface Review and Letters, 1996, 03, 157-160.	0.5	1
650	Surface Functionalization of Silicene. Nanoscience and Technology, 2018, , 211-233.	1.5	1
651	Insight into void formation near grain boundary from phase-field simulations. Nuclear Instruments & Methods in Physics Research B, 2019, 453, 50-55.	0.6	1
652	Structural and Electronic Properties of Binary Clusters Si _{<i>m</i>} Ge _{<i>n</i>} (<i>m</i> + <i>n</i> = 6–13). Journal of Nanoscience and Nanotechnology, 2019, 19, 7879-7885.	0.9	1
653	Phase Diagrams for sII Clathrate Hydrates of CO2 from First-Principles Thermodynamics. Journal of Physical Chemistry A, 2021, 125, 5956-5962.	1.1	1
654	Remote Passivation in Two-Dimensional Materials: The Case of the Monolayer–Bilayer Lateral Junction of MoSe2. Journal of Physical Chemistry Letters, 2021, 12, 8046-8052.	2.1	1
655	Hydrogen Adsorption and Penetration of Cx (x=58-62) Fullerenes with Defects. Lecture Notes in Computer Science, 2007, , 280-287.	1.0	1
656	Surfaceâ€enhanced resonance Raman detection of 1,1â€diaminoâ€2,2â€dinitroethylene (FOXâ€7) on metalâ€do 12 and Ag 12 clusters. Journal of Raman Spectroscopy, 2020, 51, 2425-2434.	oped Au 1.2	1
657	Cluster- and energy-separated extreme states in a synthesized superatomic solid. Physical Review B, 2022, 105, .	1.1	1
658	Strain softened bending modulus of graphene oxide. Carbon Trends, 2022, 7, 100167.	1.4	1
659	Numerical methods for efficient GW calculations and the applications in low-dimensional systems. Electronic Structure, 0, , .	1.0	1
660	Conductance resonance of coupled supported metal clusters. Physics Letters, Section A: General, Atomic and Solid State Physics, 1995, 204, 291-294.	0.9	0
661	The effect of interaction between supported Au clusters on the conductance resonance. Journal of Applied Physics, 1995, 78, 3528-3530.	1.1	0
662	Endohedral Silicon Fullerenes SiN (27 ≇ â‰z39). ChemInform, 2005, 36, no.	0.1	0
663	TRANSITION METAL/CARBON NANOTUBE HYBRID STRUCTURES. International Journal of Nanoscience, 2005, 04, 139-147.	0.4	0
664	Fluctuations of tensile strength and hardness of c-BC ₂ N crystals induced by difference in atomic configuration. Journal of Physics Condensed Matter, 2011, 23, 465401.	0.7	0
665	Application of GO in Energy Conversion and Storage. SpringerBriefs in Physics, 2015, , 79-118.	0.2	0
666	Charge effect on the irradiation damage of silicon: Insights from phase-field simulation. Materials Today Communications, 2020, 24, 101187.	0.9	0

#	Article	IF	CITATIONS
667	First-Principles Study of the Effects of Carbon, Nitrogen, and Oxygen on Helium Behavior in Body-Centered-Cubic Vanadium. Fusion Science and Technology, 0, , 1-10.	0.6	0
668	Improved stability of water clusters (H2O)30–48: a Monte Carlo search coupled with DFT computations. Highlights in Theoretical Chemistry, 2012, , 75-81.	0.0	0
669	First-principles study of crystal-face specificity in surface properties of Fe-rich Fe-Cr alloys. Physical Review Materials, 2019, 3, .	0.9	0
670	Enhanced ferromagnetic ordering of Mn trimer symmetrically and fully exposed on iridium-doped graphene. Journal of Physics B: Atomic, Molecular and Optical Physics, 0, , .	0.6	0
671	Interlayer Hopping Kinetics of Vacancies in Crl ₃ Layers Leading to Monolayer/Bilayer Heterostructures. Advanced Materials Interfaces, 0, , 2200626.	1.9	0